SKB TECHNICAL REPORT 93-10

Mechanisms and consequences of a creep in the nearfield rock of a KBS-3 repository

Roland Pusch, Harald Hökmark

Clay Technology AB, Lund, Sweden

December 1992

SVENSK KÄRNBRÄNSLEHANTERING AB
SWEDISH NUCLEAR FUEL AND WASTE MANAGEMENT CO
BOX 5864 S-102 40 STOCKHOLM
TEL. 08-665 28 00 TELEX 13108 SKB S
TELEFAX 08-661 57 19

MECHANISMS AND CONSEQUENCES OF CREEP IN THE NEARFIELD ROCK OF A KBS3 REPOSITORY

Roland Pusch, Harald Hökmark

Clay Technology AB, Lund, Sweden

December 1992

Mechanisms and Consequences of Creep in the Nearfield Rock of a KBS3 Repository

Lund, December 1992

Roland Pusch
Harald Hökmark

Clay Technology AB
IDEON, 22370 Lund
Sweden

MECHANISMS AND CONSEQUENCES OF CREEP IN THE NEARFIELD OF KBS3 TUNNELS AND CANISTER HOLES IN GRANITIC ROCK

Roland Pusch
Harald Hökmark

December 1992

Keywords: Creep, energy barrier, energy spectrum, Griffith voids, Kelvin model, load tests, log time creep, rock discontinuities, rate process theory, rock structure, strain, strain rate, stress, temperature

ABSTRACT (ENGLISH)

Creep in rock depends on the structure as well as on the stress and temperature. Log time creep is often observed and can be explained on the basis of statistical mechanics. Simple Kelvin behavior can be used as an approximation. The code FLAC is concluded to be useful for predicting creep strain, assuming that the rock obeys the Kelvin law.

ABSTRACT (SWEDISH)

Krypdeformationer i berg beror av bergets struktur liksom på spänningen och temperaturen. Logaritmiska tidsberoenden observeras ofta hos kryprörelser och kan förklaras på basis av statistisk mekanik. Reologiska element av Kelvin-typ kan användas som approximation. Koden FLAC konstateras vara användbar för att prediktera kryprörelser, förutsatt att berget uppför sig som ett Kelvin-material.

LIST OF CONTENTS

SUMMARY

Creep is associated with microcracking in small elements of structurally homogeneous crystalline rock, while slip along weak planes is responsible for time-dependent deformation of structurally heterogeneous rock. The major process leading to the latter type of creep is stepwise displacement of microscopic slip units when the activation energy for slip is exceeded. Since the barriers represent a large spectrum of energies, macroscopic creep strain is a function of both stress, temperature and time. It can be shown theoretically that when the structure is not altered the creep strain should be proportional to the logarithm of time, and this is also a commonly observed rate in loading tests and excavation of tunnels.

A pilot FLAC study is presented, in which the Kelvin rheological model has been used to approximate time dependent material behavior of homogeneous rock surrounding a circular tunnel in a biaxial stress field. The horizontal to vertical stress ratio is 2.5. A 0.5 m deep zone around the tunnel periphery is assumed to exhibit creep behavior. The calculation shows that the numerical tool used for this study has a good potential of describing time dependent processes in a meaningful way. Time scales and orders of magnitude are in good agreement with the numerical input. For a 2.4 m diameter tunnel the inward displacement of the periphery is found to be about 0.3 mm. The creep strain in the roof, i.e. where tangential stresses are high, is one order of magnitude larger than in the walls.

1 INTRODUCTION

Commonly, rock mechanical exercises only require application of very simple material models, disregarding the influence of time on rock strain. Still, successful treatment of a number of practically important problems implies that the time lag is considered in the calculations, common examples being settlement of heavy structures, displacement of heavily pressurized linings in gas storages, interaction between unstable rock and supporting constructions, and long-term roof stability in large rock caverns. In such cases the creep behavior of rock may have to be taken into account, still recalling that the usually very complex physico/chemical processes that govern time-dependent strain have to be represented by rather simplified rheological models. Some of the basic considerations herein will be presented and discussed in this report, which is focussed on crystalline rock. We will see that scale factors play a major role, meaning that the rock structure needs to be considered as a major factor.

2 FUNDAMENTALS OF CREEP IN ROCK

2.1 GENERAL

The term creep is commonly used to describe all sorts of time-dependent deformation, extending from large-scale crustal strain to deformation of discrete crystals exclusively due to well defined dislocation glide, with an intermediate spectrum of movements that depend on structural features and scale factors.

As when solving other rock mechanical problems, the structural and mineralogical heterogeneities imply that the selection of rheological parameters must be made with due respect to the strain-controlling features. Sedimentary and metamorphic rocks often exhibit significant creep that affects the stability of rock caverns, while hard igneous rock usually shows insignificant short-term creep on loading or unloading. Still, even in such rock, time-dependent strain accumulates in the roof of tunnels and the walls of shafts and may ultimately yield rock fall and collapse. The matter is of special importance for oil, gas and hot water storages as well as for repositories for depositions of hazardeous waste products, since time-dependent strain in the form of increased aperture and connectivity of fractures may raise the hydraulic conductivity of the near-field rock. Proper formulation of design criteria and selection of suitable techniques for rock stabilization require some understanding of the involved mechanisms, which we will examine before considering the possibility of formulating theoretical and empirical creep models.

2.2 PROCESSES LEADING TO CREEP STRAIN

The nature of creep in rock is very much dependent on the mineralogical composition and microstructural constitution, as well as on whether the strain takes place within the crystal matrix or along preexisting fractures. Thus, as in the case of rock strength and failure, there are considerable differences in the behavior of small samples tested in the laboratory and of larger rock volumes (1,2).

A frequently claimed opinion is that creep is associated with microcracking as concluded from microscope analyses and recording of acoustic emission. However, numerous examples have been given of creep at room temperature that is associated with formation of slip lines and twinning, indicating significant dislocation glide mobility. Halite and calcite crystals and marble rock appear to behave in the latter fashion and so do phyllosilicates, exhibiting slip along basal planes. Since calcite and phyllosilicates are common fracture-filling minerals such slip is a major mechanism in creep along fractures, while creep in the virtually isotropic, coherent crystal matrix of many crystalline rocks may be dominated by microfracturing. Temperature is a major parameter in this context and so is stress; together they determine whether the creep will have the form of strain at a constant rate, if it is rapidly retarded, or if it will be of the commonly observed transient type.

Structural heterogeneity is clearly a common feature of materials showing transient creep and various attempts have been made to explain rock creep in terms of migration and interaction of dislocations. This may well apply to the deformation of individual crystals and small crystal aggregates, but for rock elements composed of different minerals with varying stress/strain and thermal properties and with a more or less heterogeneous structure, other mechanisms control the time-dependent strain. Thus, a main source of creep of fracture-poor rock is shear displacement along crystal lattice planes and along interfaces between contacting crystals of different minerals. The latter contacts are characterized by imperfectly fitting atomic lattices at the points of mechanical interaction, and by incomplete common boundaries forming Griffith voids (Fig.1), which, together, are responsible i.a. for the porosity and capillary properties of virtually fracture-free rock. These features imply a considerable variation in bond strength, a property that is strongly scale-dependent and also largely controlled by the amount of strain. This latter factor is important for all sorts of silicates since mechanically induced exposure of free crystal surfaces causes hydration due to the hydrophilic potential yielding further dispersion, a phenomenon that is particularly important for phyllosilicates like the clay minerals. The larger the rock

mass, the more important are fissures and fractures for the rheological behavior in bulk. Especially their mineral coatings and infillings and "topography" are determinants of much of the practically important creep in rock.

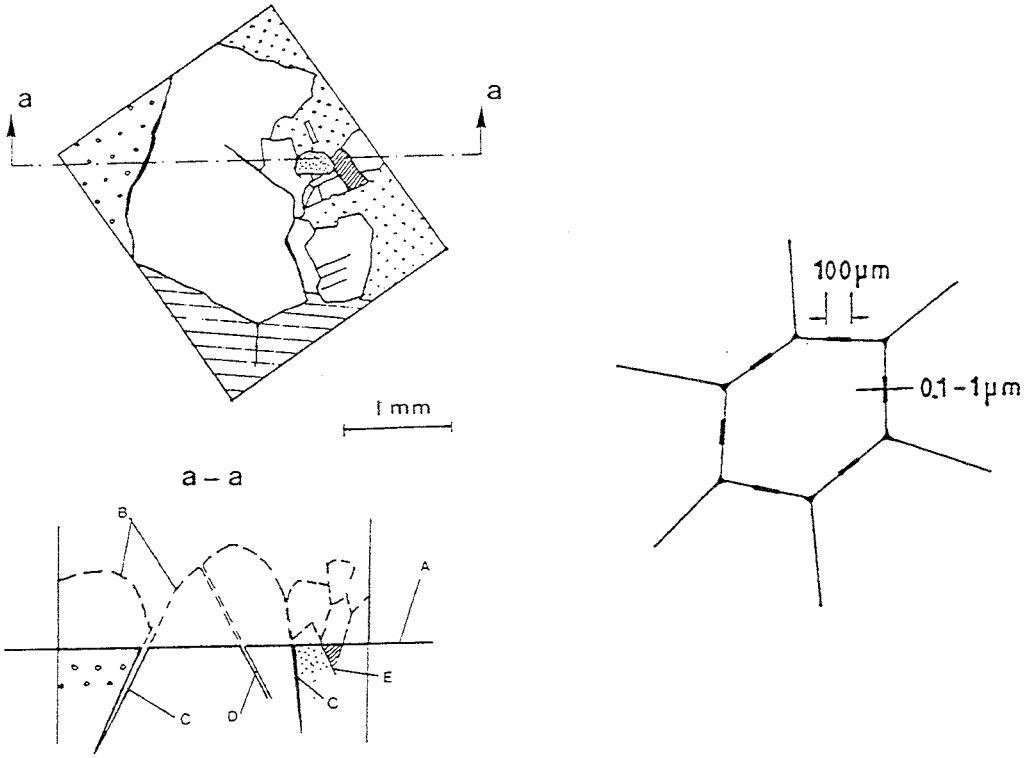

Figure 1 Griffith-type voids in the crystal matrix. a-a is a cross section with A) representing a polished thin section surface, B) the actual irregular surface of a joint, C) incomplete crystal contacts, D) fissure, and E) tightly contacting crystals. The right picture shows generalized microscopic breaks termed 7th order discontinuities (1)

3 FORMULATION OF CREEP STRAIN

3.1 TEMPERATURE DEPENDENCE

Rock creep is temperature-sensitive, which means that it is basically a thermally activated process (2). Keeping in mind also the polycrystalline nature of the rock with a very large number of differently mobilized crystal bonds, it is logical to apply the concept of molecular jump activation and rate process theories in the mathematical formulation of creep in rock. It implies that displacements are considered as thermally assisted passages over energy barriers aided by the application of stress. This approach has been made by various investigators, covering the entire range from small rock elements, like single crystals or polycrystal aggregates, to many cubic meters of rock for which the creep is due to displacements along one or a few discontinuities.

By tradition and convenience rock scientists distinguish between viscoelastic creep, being largely recoverable on unloading, partly recoverable low-temperature creep, and non-recoverable high-temperature creep, which is usually but not always transient. It has been suggested on empirical grounds that purely viscoelastic creep at low temperatures is limited to a strain less than 10^{-4} and related to movement along pre-existing cracks, and that non-recoverable creep at intermediate temperatures, i.e. between room temperature and $\underset{\sim}{0}.3\ T_m$ where T_m is the melting temperature ($\approx$2000 K) stems from dislocation glide with low diffusion rates (1). Creep at temperatures exceeding 0.5 T_m is usually of the steady-state type when it is not recoverable, and transient when it is recoverable.

3.2 CREEP MECHANISMS

The variation in physical interaction between neighboring crystals means that there is a strength spectrum over a cross section of any size, suggesting that statistical mechanics can be used for describing creep in rock. Basically, creep is produced by the continuation of the slip process initiated by the activation and formation of slip units. The major strain-generating mechanisms, which are strongly scale-dependent are:

* Application of a sufficiently high shear stress initiates slip, i.e. local plasticity, in the form of translatory shear displacements at overstressed crystal contacts and along certain atom planes in individual crystals, as well as slip at the interface between contacting asperities in fissures and fractures

* Redistribution of microstresses is facilitated by slip, by which higher local stresses are produced where they were previously relatively low. This causes local stress increase and additional microstructural plasticity by which the creep rate is *enhanced*.

* Deformation will induce local displacements such that stronger units will make contact and help to strengthen the structure. This involves micro-dilatancy and mechanical interlocking, which, together with precipitation and pressure solution are the main "healing" processes by which the creep rate is *retarded*.

The net effect of the listed mechanisms depends on the magnitude of the deviator stress and the total strain. Sufficiently high stresses produce accumu-

lated structural breakdown by which the damaging processes outweigh the healing ones and the strain rate increases and ultimately yields failure. At lower stresses, short-term creep is retarded but geometrical conditions yielding dilatancy or offering restraint, control the macroscopic behavior. Thus, if dilation is prevented or minimized, as when applying heavy loads to foundations resting on rock at some depth below the ground surface, the number of activated slip units is largely constant and the creep decelerates, while if expansion takes place as in the case of a rock wedge that is free to slip from a tunnel wall, disintegration eventually occurs and the number of slip units decreases.

3.3 EMPIRICAL CREEP LAWS

In practical engineering a number of empirical and theoretically derived creep laws have been introduced for quantitative description of rock creep at low temperatures. Most of them can be expressed in the form:

$$\dot{\varepsilon}(t) = A \cdot t^{-n} \quad (0 \leq n \leq 1) \qquad (1)$$

where $\dot{\varepsilon}(t)$ is the creep strain rate and A and n constants that depend on the material as well as on the test conditions. n = 1 gives the logarithmic creep law, which seems to be generally applicable at stresses lower than 2/3 of the failure stress and at temperatures lower than 0.2 T_m (2,3,4). Andrade-type creep with n = 2/3 has been frequently observed at higher stresses and temperatures. Typical log time creep behavior is illustrated in Fig.2.

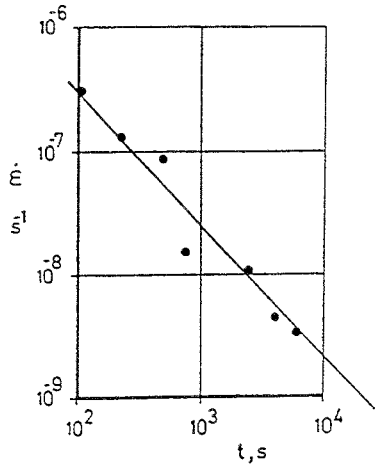

Figure 2 Typical creep record for granite, exhibiting almost perfect log time behavior (4)

Many experiments have shown a more rapid decay in creep rate than implied by the log t and Andrade laws. They appear to be typical of small samples exposed to low deviatoric stresses, a typical example being given in Fig.3.

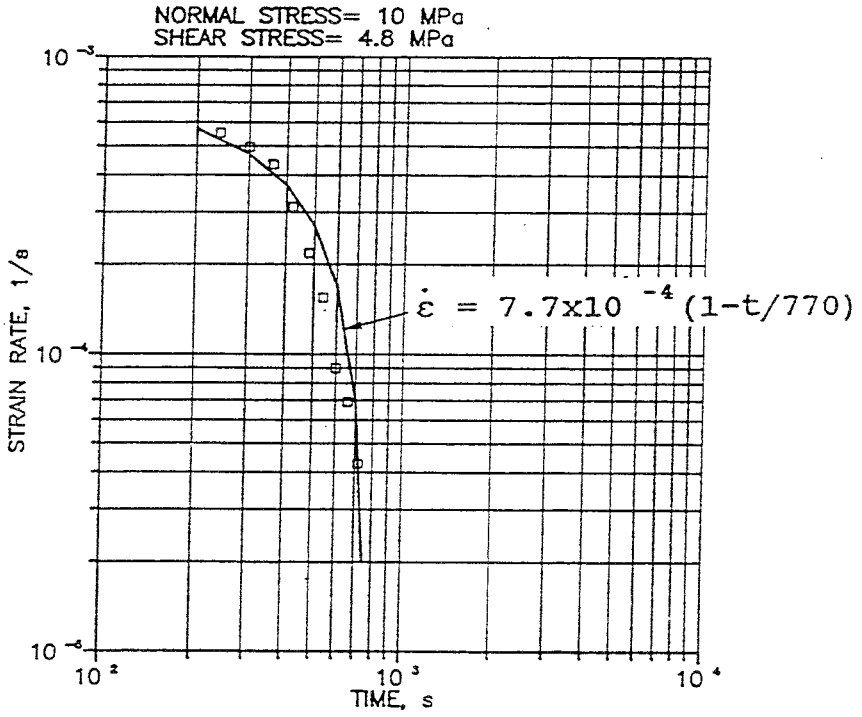

Figure 3 Strongly retarded creep of chlorite shale in shear box test. Normal stress 10 MPa, shear stress 4.8 MPa

3.4 RATE PROCESS THEORY

3.4.1 Steady state creep

Steady state creep can be expressed in the following form:

$$\dot{\varepsilon} = A \exp(-U/RT) f(\sigma) \qquad (2)$$

where A = Temperature-dependent constant
U = Creep activation energy
R = Universal gas constant
T = Temperature
$f(\sigma)$ = Stress function

There are indications that U is related to the diffusivity of the least mobile atomic species (5), which means that diffusion may control the creep rate. This supports the opinion that dislocation

climb theories are applicable in explaining the nature of certain types of creep.

Literature provides a large number of attempts of relating experimentally determined creep data to various creep models based on Eq.(2), a comprehensive treatment being given by Carter & Kirby (6).

3.4.2 Transient, retarded creep

Most creep curves representing experiments at low temperatures and stresses exhibit a monotonically decreasing strain rate, which is in agreement with the following physical model:

1. There is a variation in activation energy for slip.
2. Each rock element contains a certain number of slip units in a given interval of the activation energy range.
3. In the course of the creep, the low energy barriers are triggered early and new slip units come into action at the lower end of the activation energy spectrum. This end represents a "generating barrier", while the high end is an "absorbing barrier".
4. When atomic jumps take place, they bring the given slip unit up against a barrier by a certain amount higher than previous one.
5. A change in deviator stress changes the rate of shift of the energy spectrum to higher u-values.

The corresponding mathematical form can be derived by considering an element subjected to a constant, intermediate deviator stress. The number of barriers of height u is taken to be $n(u,t)\delta u$, where δu is the energy interval between successive jumps of a slip unit, and t the time. As a first approximation, the initial distribution $n(u,0)$ at the application of the stress can be taken as constant as represented by the "box-shape", i.e. the broken line in Fig.4.

$$n(u,0) = \text{const.}, \qquad u_1 \leq u \leq u_2 \tag{3}$$

The change of the activation energy in the course of creep means that the number of slip units is determined by the outflux from any u-level into the adjacent higher energy interval and by a simultaneous influx into the interval from $u-\delta u$.

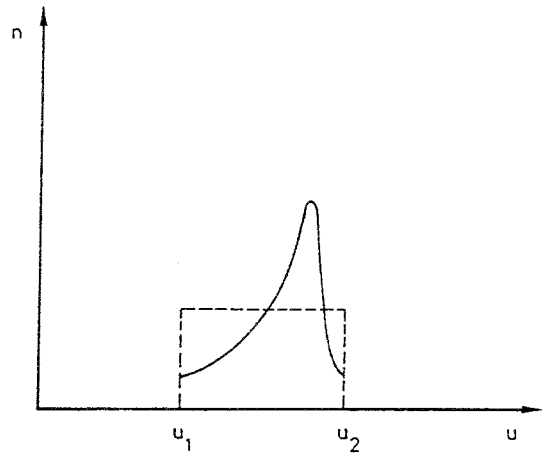

Figure 4 Activation energy spectrum at a given time after the onset of creep. Broken curve shows simple "box shape"

Following (7) and (8) we obtain the following expression for the rate of change of n(u,t) with time:

$$\partial n/\partial t = -(\nu\delta u)\partial[n \exp(-u/kT)]/\partial u \qquad (4)$$

where δu = width of an energy spectrum interval
ν= vibrational frequency (10^{12} s^{-1})
k = Boltzmann's constant
T = Absolute temperature

By introducing a transition probability density N to describe the time-dependent energy shift one obtains:

$$N(u,t) = n(u,t)\exp(-u/kT) \qquad (5)$$

By putting r = exp(u/kT) we find:

$$\partial N(r,t)/\partial t = -D\partial N(r,t)/\partial r \qquad (6)$$

where $D = \nu\delta u/kT$

The solution of Eq(6) is of the type:

$$N = \phi(r-Dt) \qquad (7)$$

where ϕ is a function of n, t and T

This expression is of the "travelling thermal front" type with the shape of N remaining fixed, but its magnitude changing with time. One possible, simple N-spectrum is shown in Figs.5 and 6, from which we have:

$$N = N_o\,[(r-Dt)^o + C(r-Dt)^1] \qquad (8)$$

where C = const., $r_1 \leq r \leq r_2$ $\quad N(u,t)>0$

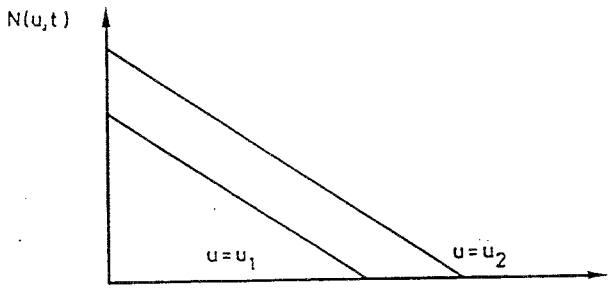

Figure 5 Example of transition probability density versus time

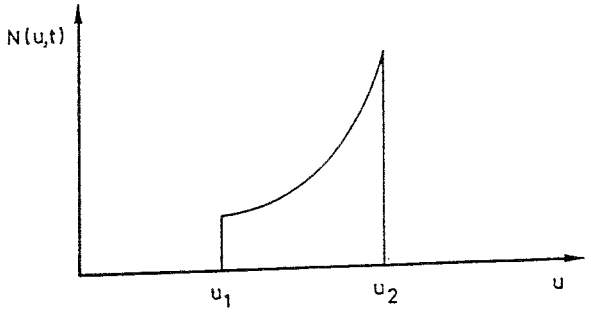

Figure 6 N(u,t) distribution for t = constant

The criterion that low barriers are triggered early in the creep is allowed for by this model. Thus, for small r-values n will decrease rapidly for a given t, compared with n-values for larger u.

If each transition of a slip unit between consecutive barriers gives the same contribution to the bulk strain, the shear strain rate is proportional to the integral of N(u,t) over the available u-spectrum. This yields the creep strain rate:

$$\dot{\gamma} \propto \int_{u_1}^{u_2} N(u,t)\,du \qquad (9)$$

and, explicitely, by applying Eq(8):

$$\dot{\gamma} \propto (1-t/t_o) \qquad (10)$$

with $t \leq t_o$ as boundary condition.

The appropriate constant of proportionality and the value of t_o depend on the deviator stress, temperature and structural details as well as on the preceding history of the slip process.

The creep is concluded to be of the form:

$$\gamma = \alpha t - \beta t^2, \quad (t \leq \alpha/2\beta) \qquad (11)$$

i.e. it starts off linearly and then dies out. Fig.3 is an example of such behavior.

3.4.3 Transient creep of common type

The log time and Andrade creep types are most commonly observed at stresses exceeding 1/3 of the shear strength. The less rapid retardation of the creep rate is explained by additional features of the physical model. They are included in the more complete and generally applicable form of the physical model that is defined below:

* The structural heterogeneity and strength variation mean that there is a variation in activation energy for slip as indicated in Fig.4. The lower boundary may represent hydrogen bonds operating between smectite, mica and chlorite flakes, while the upper boundary corresponds to primary valence bonds of unfractured crystal lattices. The spectrum will vary in the course of the creep so that some energy barriers become enhanced due to locally dropping shear stresses, while others become operative through local stress rise.

2. Each rock element contains a number of slip units in a given interval of the activation energy range at each particular time after the onset of the creep.

3. In the course of the creep, new slip units are generated at the lower end of the energy spectrum, while the high u-end is an "absorbing barrier".

4. Jumps bring the given slip unit up *or down* against a barrier by an amount δu higher *or lower* than the previous one.

A basic assumption is that the attempt frequency of slip $\nu(u)$ is given by the Arrhenius rate equation:

$$\nu(u) = \nu_D \exp(-u/kT), \qquad u_1 \leq u \leq u_2 \tag{12}$$

where u is the barrier height. Here, ν_D is an atomic vibrational frequency of the order of 10^{12} s^{-1}.

If slip has been activated at a certain point in the crystal matrix, i.e. a barrier has been overcome, a contribution to the overall shear is made by the associated extension of the local slip-patch. The next barrier to be encountered by the same spreading slip zone will be either higher or lower by an average amount δu. The magnitude of δu is determined by the amplitude of the internal stress field and by the physical nature of the barriers.

Assuming an equal probability of slip, meaning that an activated jump of a patch brings it to a barrier which is either lower or higher than the previous one, the following relationship can be derived:

$$\partial n/\partial t = D\{\partial^2[n \exp(-u/kT)]/\partial u^2\}$$

$$D = \tfrac{1}{2}\nu_D(\delta u^2) \tag{13}$$

where t = time after onset of creep and where n is short for n(u,t).

If the attempt frequency of all such points is $\nu_D e^{-u/kT}$, then the contribution by the u-interval to the flow rate in uniaxial tension or compression is:

$$\delta\dot{\varepsilon} \propto \nu_D n(u,t) \exp(-u/kT)\delta u \tag{14}$$

Now, if it is assumed that each activated jump makes the same, average contribution to the bulk strain, the rate of creep will be:

$$\varepsilon \propto \int_{u_1}^{u_2} e^{-u/kT} \cdot n(u,t)\,du \tag{15}$$

which yields the relationship

$$\varepsilon \propto 1/(t+t_o) \tag{16}$$

where t_o is an integration constant. We immediately see that this is the log time creep law, which can thus be derived theoretically.

3.4.4 Influence of stress and temperature

The appropriate constant of proportionality in Eq(16) depends on the deviator stress, temperature, and structural details. Within a narrow stress interval, well below the failure level but also significantly

above that characterized by rapidly retarded creep, the frequency of activated slip units should be approximately proportional to the applied stress, yielding a roughly linear relationship between stress and creep rate. For an ambient temperature up to about 100°C the influence of heat is known to be very small and for this interval an approximately linear relationship between absolute temperature and creep rate is probable. Assuming linearity in stress and temperature Eq(16) yields:

$$\dot{\varepsilon} \propto T\sigma/(t+t_o) \text{ with } \sigma = \text{const.} \qquad (17)$$

where t_o depends on the structure, stress history, and mineralogical composition.

The meaning of Eq (17) is that the creep rate is successively retarded as a consequence of the "blue-shift", i.e. displacement of the activation energy spectrum towards higher levels, that results when the strengthening processes outweigh the damaging ones.

While linear dependence of strain rate upon stress, yielding Newtonian viscosity, is typical of steady state creep of the earth's mantle (Nabarro-Herring or Coble creep), the strain rate of interest to engineers depends upon a higher power of the stress (9). For instance, this is the case for all types of dislocation migration. Thus, a number of independent studies indicate that the creep rate is proportional to σ^n, where n usually ranges between 3 and 7. This strong stress dependence is not accounted for by any perfectly logical theoretical model.

As to the influence of thermal treatment, it is true that heating from room temperature to around 100°C does not affect the creep rate significantly but beyond this limit the influence becomes obvious, especially at high stresses (1,2), cf.Fig.7. Ongoing research suggests that mechano/chemically induced alteration of minerals may be a common phenomenon in shear zones even at low temperatures, implies that shifts in the energy spectrum are very complex.

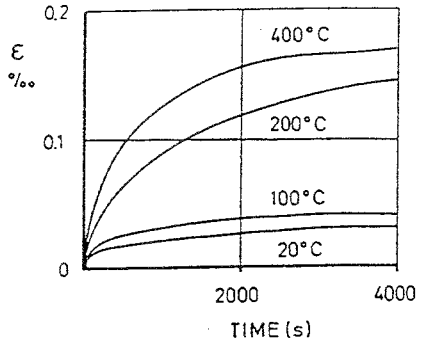

Figure 7 Example of laboratory-determined creep strain of granite samples at uniaxial compression and varying temperature

It is worth noting that the influence of heat indicated in Fig.7 is of significant practical importance. Thus, one finds that the substantial increase in creep strain on heating from room temperature to more than 100°C will lead to appreciable block movements and to a considerable permanent increase in hydraulic conductivity (10).

4 RECORDINGS

4.1 LABORATORY TESTS

In the transient creep regime, log time creep approximately linear in stress and temperature as expressed by Eq(17), is widely observed in experiments with rock material of all kinds. Thus, under uniaxial compression, many small cored samples tend to obey this creep law as long as the stress is in the interval 1/3 to 2/3 of the conventionally determined failure stress (Fig.8). Still, many transient creep data also fit power laws, the accuracy of the measurements on small intact samples often being too low to identify the best-fitting law.

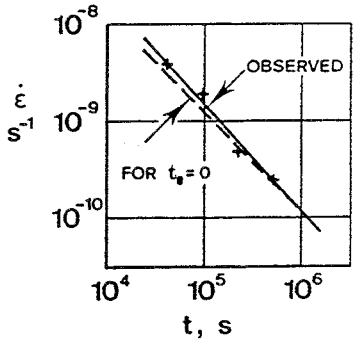

Figure 8 Creep behavior of uniaxially loaded granite drill core exhibiting log time creep rate with slight negative t_o. The axial stress corresponded to 40 % of the compression strength

4.2 FIELD LOAD TESTS

Measurement of settlements of foundations on rock have been used by several investigators to determine the creep properties of the bedrock and such recordings turn out to be valuable when the rock consists of soft shales, limestone and the like. For crystal-

line rock, however, the prerequisites for conducting meaningful and sufficiently accurate measurements are seldom at hand in field testing, since the strain is small and the influence of temperature variations and other disturbances usually considerable. Still, two studies of reasonable accuracy have been reported, of which one concerned loading tests of the walls of blasted tunnels in granite, yielding the strain and strain rates - clearly of log time type - given in Fig.9 (11).

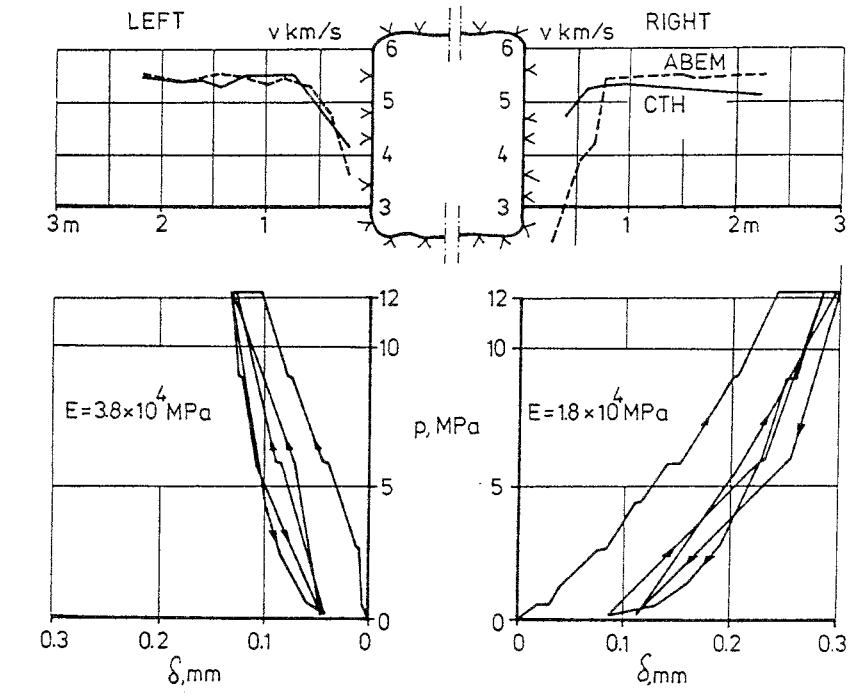

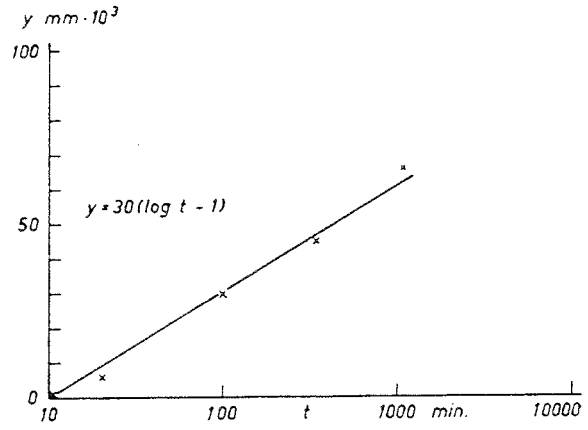

Figure 9 Plate loading of the walls of blasted tunnel in granite. Upper picture shows recorded strain at cyclic loading, and wave velocity applying seismic (ABEM) and ultrasonic (CTH) techniques. Lower picture shows creep at constant load (11)

The other case concerned plate-loading tests on biotite-rich, slightly weathered gneiss with a marked subhorizontal layer-type structure (12). It demonstrated the applicability of the log time law with a rather high t_o-value (Fig.10). The test arrangement, which is shown in Fig.11, made it possible to record the settlement of cylindrical foundations with a radius of 0.35 to 1.0 m and a maximum average pressure of about 100 MPa. The load was applied in 1 MPa steps.

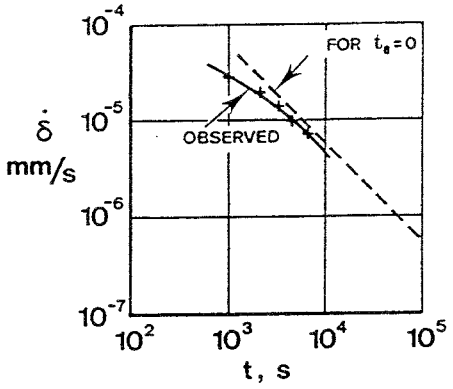

Figure 10 Settlement rate at plate-loading test on gneiss showing successive approach to log time strain rate. Contact pressure 42 MPa

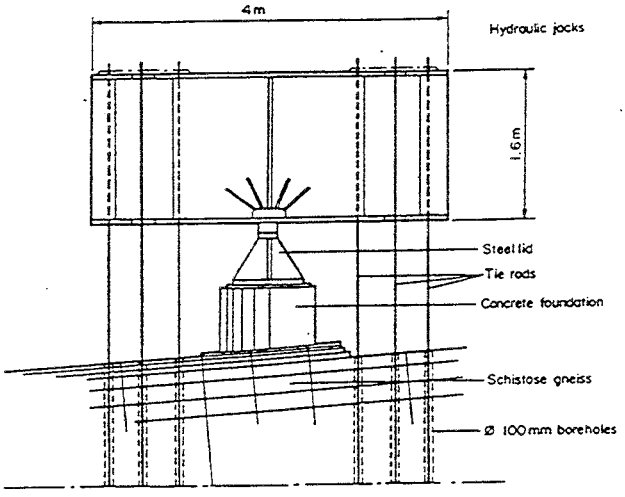

Figure 11 Arrangement for plate-loading tests

4.3 OTHER FIELD RECORDINGS

Several convergence measurements in tunnels have given information on the time-dependence of creep in larger volumes of rock. Most recordings appear to fit

the log time law but the recording time was certainly not sufficient to give safe information on the validity of this law over longer periods of time (13,14). Actually, the strain rate must be expected to increase sooner or later because of the ultimate softening of the rock that results from dilatancy and loosening of shallow blocks. Applying the terminology of microstructural creep processes, such changes in the continuity of a rock mass can be expressed as an altered population and character of slip units. Yet, it is interesting to see that the log time creep law is applicable also to large rock masses, implying that they behave according to statistical mechanics as do the small rock elements.

Summing up, it appears that both theoretical considerations and many recorded creep rates indicate that the log time law is of general applicability for viscoelastic as well as viscoelastoplastic material undergoing non-recoverable strain. For rock material with recoverable viscoelastic strain the Kelvin rheological model has occasionally been used (1). One example is the estimation of future time-dependent strain of the Forsmark rock hosting the big silo with radioactive waste products (15). We will return to this latter possibility in a later chapter dealing with numerical calculations.

5 CREEP OF ROCK IN KBS3 TUNNELS AND CANISTER DEPOSITION HOLES

5.1 MAJOR FACTORS

It is clear from the preceding treatment of the subject that the theoretical creep model based on stochastical mechanics and manifested by the log time creep law is only valid if the number of slip units does not decrease in the course of creep strain, requiring that the rock mass has its structure preserved in the course of the creep and that it does not undergo expansion and disintegration. This condition is valid if the ambient, confining pressure is high enough, which requires that the support offered by the buffers and backfills must be sufficient in the case of KBS3 tunnels and depositions holes. If so, the creep strain will be retarded and fade off in a long term perspective. If not, the rock will undergo expansion and drop in strength yielding unstable conditions with highly increased hydraulic conductivity, creep failure and rock fall. We will investigate these matters in the present chapter by considering the near-peripheral rock in canister deposi-

tion holes filled with highly compacted bentonite, and the roof of blasted KBS3 tunnels. The two cases involve largely different rock volumes with very different structural features and we therefore need to start the discussion by defining these features.

5.2 ROCK STRUCTURE

5.2.1 Characterization

Strength and strain phenomena are basically related to the rock structure for which a general rock classification scheme (GRS) has been introduced (16). It covers a large spectrum of discontinuities, ranging from major faults to Griffith voids and we will use it when describing rock strain and failure in this report. The scheme distinguishes between multi-fracture discontinuities, "fracture zones", of 1st to 3rd order and high-order discontinuities in the form of hydraulically active discrete fractures or joints of long extension (4th order), and "latent" fractures (5th order), which can all be seen with the unaided eye (Fig.12). These discontinuities form more or less regular patterns with subsystems of microscopic defects of which stone-cutters make use in preparing cubical pavement blocks of seemingly homogeneous and isotropic granite. This latter type is termed 6th order discontinuities. The smallest defects, the Griffith voids (Fig.1), are randomly oriented in intact rock crystal matrix. (7th order)

5.2.2 Strength and stress/strain properties of minor discontinuities in undisturbed rock

For the present purpose we do not need to consider the low-order discontinuities since they will hardly interfere with the more sensitive parts of a KBS3 repository. The high-order structures, on the other hand, will control the stability and thereby the strain of such parts, of which the strength parameter values in Table 1 are representative (16). No true cohesion is assumed for any of the discontinuities.

Table 1 Angle of internal friction of high-order discontinuities

Discontinuity	Angle of internal friction, degrees	
	Peak	Residual
4th	30-35	20-30
5th	40-50	35-40
6th	50-60	40-50

The bulk rock properties naturally depend on the type and frequency of discontinuities that are present and this gives the wellknown influence of scale on these properties. Applying the Mohr/Coulomb failure theory and the average spacings and extensions of discontinuities that are implied by the GRS one arrives at the approximate figures in Table 2.

Table 2 Bulk shear strength parameters of undisturbed crystalline rock (16)

Rock volume m^3	Cohesion MPa	Angle of internal friction degrees		Types of discont.
		Peak	Residual	
<0-001	10 - 50	45-60	40-50	7th
0.001-0.1	1 - 10	40-50	35-45	6th, 7th
0.1-10	0.5- 5	35-45	30-40	5th, 6th, 7th
10-100	0.1- 1	25-35	20-30	4th, 5th, 6th, 7th
100-10000	0.01- 0.1	20-30	15-25	3rd, 4th, 5th, 6th, 7th
>10000	0	<20	20	All

5.2.3 Effect of excavation on the rock structure

The drilling of deposition holes is expected to create a shallow, 5-10 cm deep zone of slight mechanical disturbance in the form of displacements along existing fine fissures and formation of new ones, yielding some insignificant relaxation of the tangential and radial stresses at the periphery. Creep will take place in two fashions:

* Time-dependent strain of the crystal matrix predominantly in the form of growth of 7th and 6th order discontinuities creating creep rupture

* Time-dependent strain in the form of shearing of joints representing 5th and 4th order discontinuities that intersect the holes or are located very close to their peripheries

Excavation of a KBS3 tunnel produces a blast-disturbed zone in which 5th and 6th order discontinuities are assumed to be activated (Fig.12) and new fractures formed in the fashion indicated in Fig.13. The removal of rock by the excavation induces strain due to the altered stress field by which some strength reduction may take place but the major strength-reducing effect is assumed to be the blast-induced "damage". The net effect of the disturbance is that the bulk cohesion and internal friction drop within 0.5-1 m from the periphery even at careful blasting and that the high tangential stresses are transferred to the rock outside this zone (Fig.14).

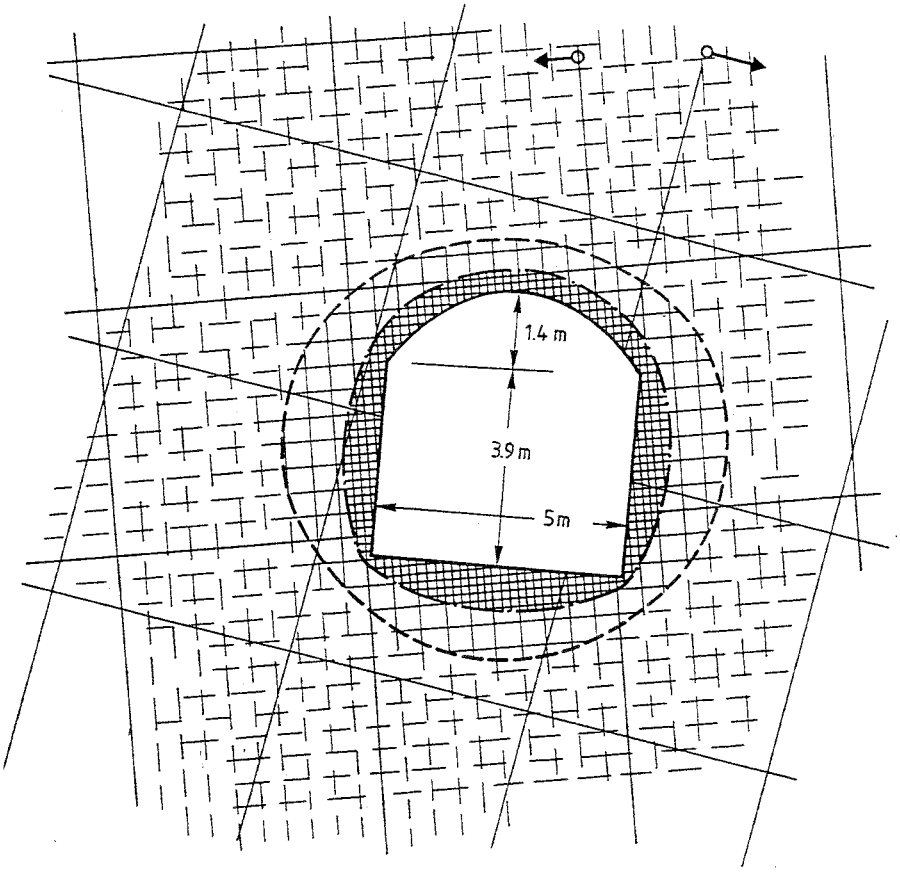

Figure 12 Cross section of blasting- and stress-induced changes in structure and rock properties. Continuous straight lines symbolize two generations of 4th order discontinuities, while the broken lines represent discontinuous, "latent" 5th order breaks that become activated within about one radius distance from the periphery. Close to the periphery there is additional damage by blasting

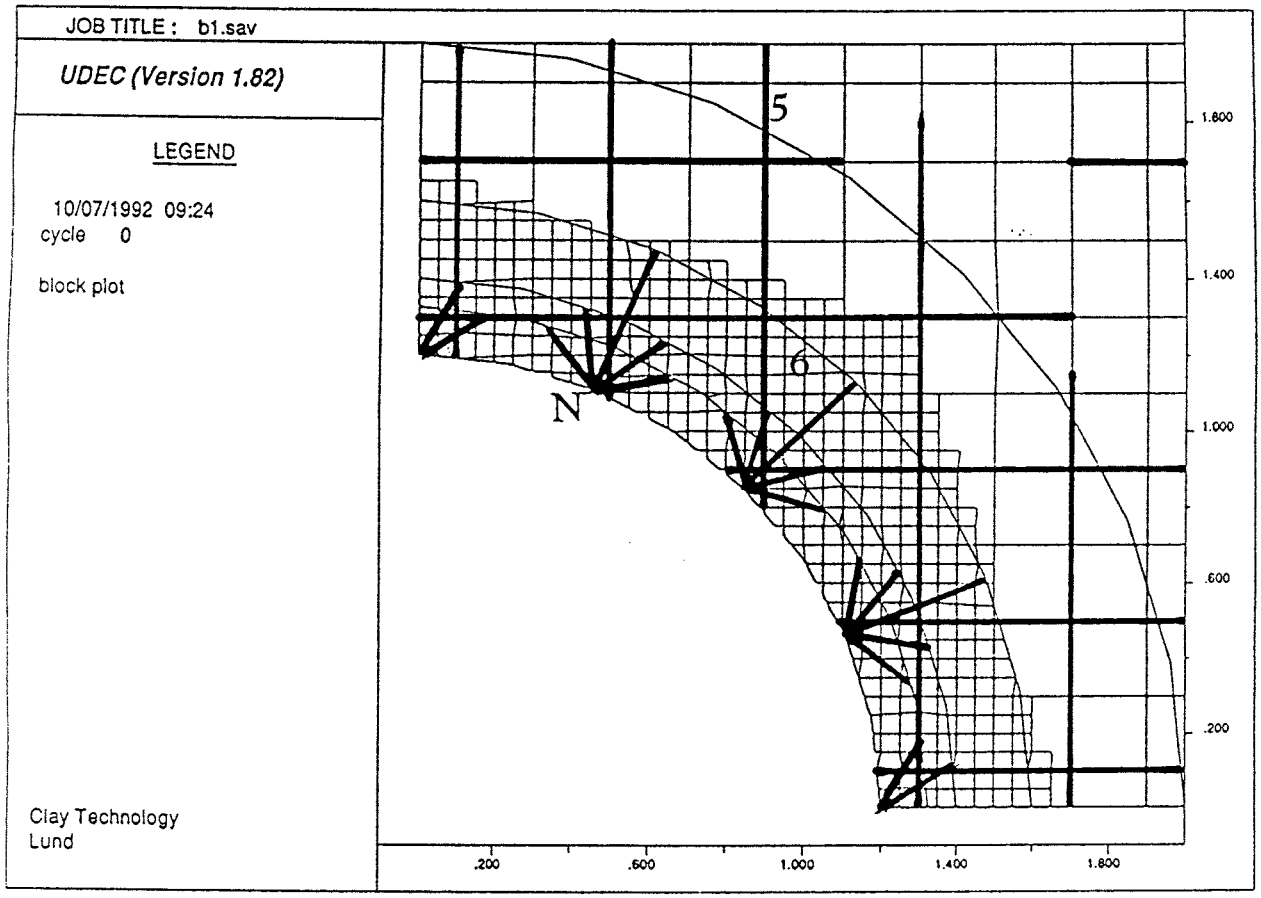

Figure 13 Model of blast-induced disturbance of the nearfield rock of a 2.4 m diameter tunnel. N are new fractures, 5 and 6 represent the respective orders of discontinuities

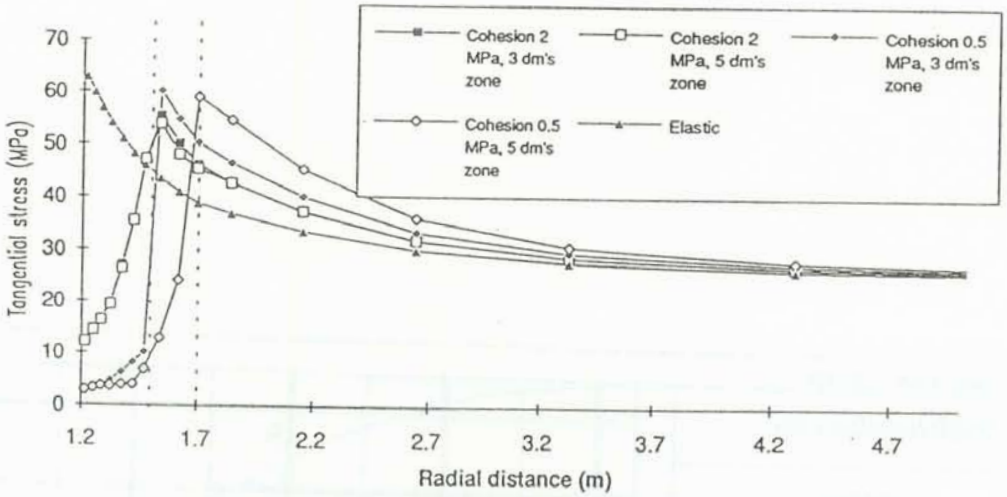

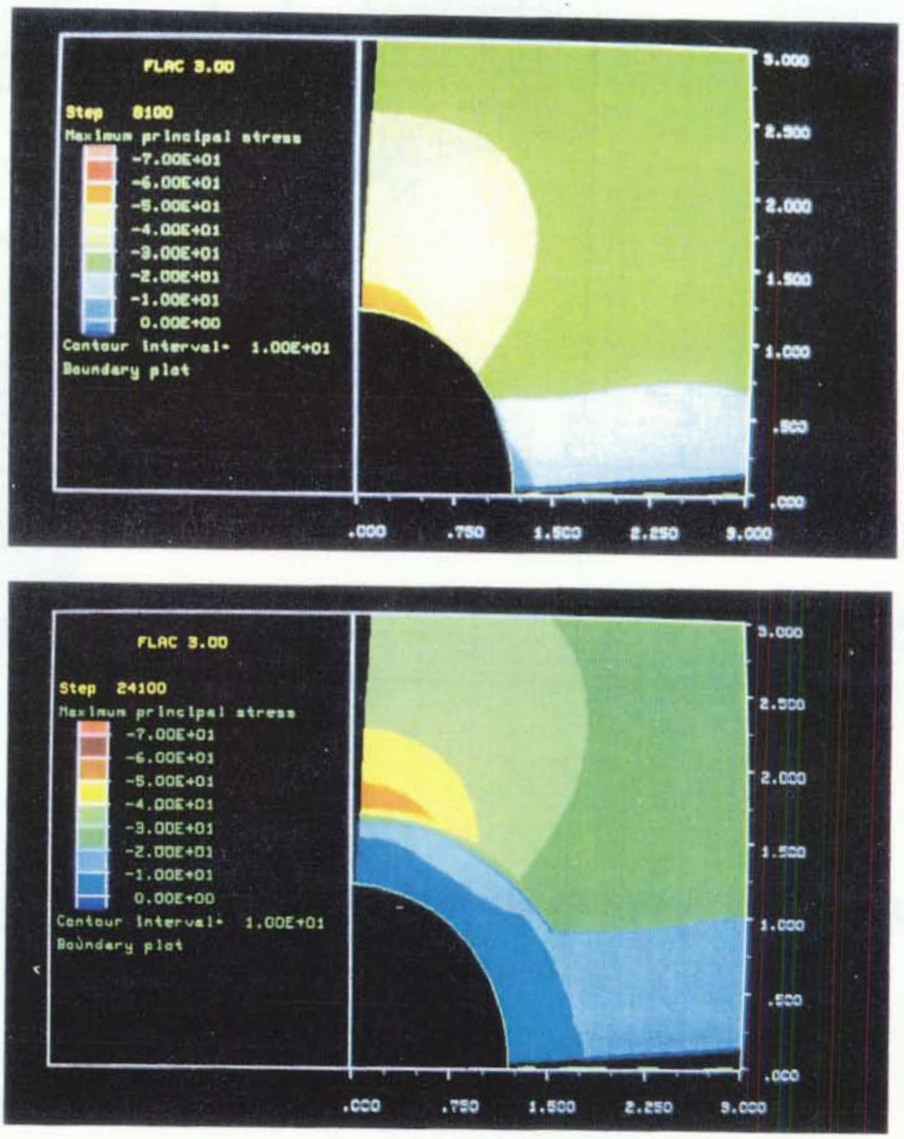

Figure 14 Upper: Effect of depth of the disturbed zone around a 2.4 m diameter tunnel on the cohesion. Lower: Contours of major principal stress for 0.5 m depth with 10 MPa cohesion (upper) and 0.5 MPa cohesion (lowest).

Creep will take place in two fashions:

* Time-dependent strain in the blast-disturbed zone by propagation of the new fractures and in the form of growth of 7th and 6th order discontinuities

* Time-dependent strain in the form of shearing of joints representing 5th and 4th order discontinuities within about 1 tunnel radius distance from the outer boundary of the disturbed zone

In principle, we find that the same types of creep will take place in the largely undisturbed rock around the deposition holes and in the excavation-disturbed roof of KBS3 tunnels. The major difference is the very large difference in frequency of discontinuities, which is manifested by the difference in bulk strength and in magnitude of the tangential stress.

5.3 CREEP STRAIN AND ITS CONSEQUENCES

5.3.1 Creep rupture mechanics

Much of our understanding of the mechanisms leading to rupture of rock materials emerges from systematic studies of the propagation of discrete cracks (17). Such studies have shown that the rate of crack tip propagation is not only a function of the stress situation and level as well as of the temperature, but also of the presence and concentration of "corrosive agents", such as moisture. Thus, material properties on the molecular scale like activation energy and activation volume are important for the appropriate mechanism of crack growth. The influence of temperature is concluded to be due to thermally activated processes ranging from simple breakage and reformation of primary valence bonds to complex chemical reactions.

It has been known for several years that freshly formed crystal surfaces are very reactive. Quartz and other silicates become hydroxylated almost instantly and aluminosilicates give off components that can form new minerals, such as smectites, in much less than one hour (18). Thus, fresh surfaces exposed in amphibole, hornblend, pyroxene, feldspar, mica, and chlorite, produced by propagating fractures, will be

hydroxylated or even coated by thin smectite films, which hydrate and exert a "disjoining" pressure. Through this the joint strength is reduced, yielding conditions for further fracture propagation. The rate of propagation is controlled by the rate of migration of water into the fracture. This type of creep rupture is expected to take place at very large depths when using bentonitic drilling muds and may be avoided by using oil-based muds.

Crack growth may take place through crystals but at low grow rates it propagates along crystal boundaries since they offer preferred paths for diffusion of reacting species like water. A common idea is that, on increasing the deviatoric stress, critically oriented microcracks and crystal boundaries grow throughout the stressed region, causing dilation (16). In the course of strain, zones will be developed along certain major directions where the crack growth and interaction is enhanced, yielding propagation of critically oriented new and pre-existing fractures. The size of load-bearing asperities in the fractures is successively reduced and, depending on the geometrical conditions, this may lead to mylonite-type structures when the strain is very large and slow, or to instant failure by shearing off asperities, which is responsible for acoustic emission in laboratory tests and for earthquake foreshocks.

An observation of general importance is that shearing of granite in triaxial tests, applying high confining pressures, yields dilation for shear stresses up to about 50 % of the shear strength (19). Such expansion is associated with brittle failure of silicates like quartz. Actually, most rock-forming silicates are brittle at low temperatures and show plastic deformation by microfracturing at this shear stress level. In contrast, calcite, micas, chlorite and pyroxene show plastic strain without microfracturing.

5.3.2 Creep rupture modelling

A number of quantitative models of creep failure have been proposed, based on criteria like crack growth to a critical length, or implying that a critical stress needs to be reached in the load-bearing contact area surrounding worn asperities. The problem is to define the critical crack length and stress, respectively, and such models are therefore of limited practical value.

Another approach that will be followed here is that the shear strength becomes uniquely reduced with the strain, which is determined by the time after onset of creep, and by the creep rate. Taking this rate to be of the log time type and the drop in strength to be linearly related to the strain, one arrives at a

very simple rule for estimating the rate of strength reduction.

The presently proposed model implies that the same destruction and loss in strength is produced by different stresses if they yield the same strain. The relation between strain and strength, for which there is much information in the literature, is here examplified by data showing that critical strain for reaching failure or very significant strength reduction is 2×10^{-4} to 5×10^{-3} (2). Fig.15 illustrates an example of recorded volumetric strain of a granite sample, showing start of dilatancy associated with comprehensive microfracturing at a compressive pressure of 250 MPa, which was about 60 % of the compressive strength. The corresponding axial strain was about 4×10^{-3} and the axial strain at complete dilatancy about 8×10^{-3}.

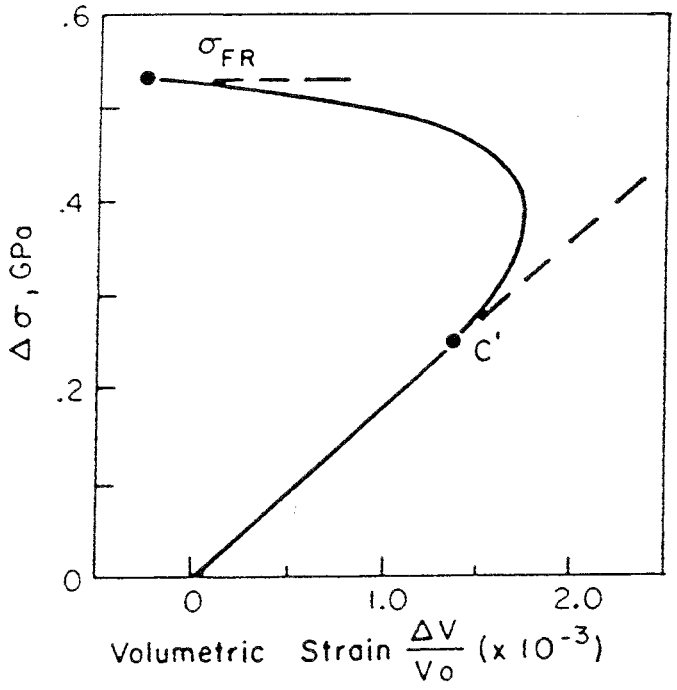

Figure 15 Volumetric strain of granite uniaxially loaded to failure. Onset of dilatancy at C′ occurred for 250 MPa compressive stress, i.e. about 60% of the compressive strength (19)

The critical strain to reach failure or very significant drop in strength is scale-dependent like all rock properties due to the successive increase in number and size of discontinuities with increasing rock volume. Hence, while the linear strain to reach

substantial microfracturing and drop in strength by 50 % or more is less than 10^{-3} for core samples, it is estimated to be twice this figure for rock volumes of several cubic decimeters, and up to $5x10^{-3}$ for volumes of one or a few cubic meters.

Thus, if laboratory experiments have shown that the peak shear strength drops by 50 % at a strain of $5x10^{-3}$ corresponding to the residual strength, and the strain is $5x10^{-4}$ for the first 10 seconds and for the subsequent 100 seconds as well as for the next 1000 seconds etc. as implied by the log time creep law, one finds that it would take somewhat more than 300 years for the shear strength to undergo such a reduction in strength. Although simple estimates of this kind only offer a very rough indication of the rate of strength reduction they are helpful in deriving general scenarios of the degradation of rock masses in which caverns, tunnels and shafts will be excavated and we will employ this line of thought in estimating the effect of creep on the rock around deposition holes and in the rock surrounding the blast-disturbed zone in the roof of KBS3 tunnels.

5.3.3 Deposition holes

Earlier calculations have shown that even in primary stress fields of high anisotropy, the maximum tangential stress will not exceed 1/4 to 1/3 of the compressive strength of the rock material (20). This means that a drop in strength that can be expected for a strain of about $5x10^{-3}$, i.e. from the peak value at short term loading to the residual strength, for instance 40 % for 5th order discontinuities and about 50 % for 6th order discontinuities (cf. Table 1), may take place in somewhat more than 300 years applying the log time creep law. Since reduction in strength will hardly proceed beyond this, we conclude that creep will not induce failure even at longer periods of time provided that hydroxylation and formation of expansive clay in the rock is limited.

Actually, even if failure conditions would be reached, the highly compacted bentonite would prevent rock fall and significant destruction of the rock at the periphery, while comprehensive fine-fracturing may take place.

5.3.4 Tunnel roofs

The long term stability of unsupported roofs of tunnels excavated in unweathered crystalline rock is a classical problem. There is sufficient evidence to conclude that such roofs may remain stable for several hundred years depending on the stress conditions,

rock structure, shape and dimensions of the tunnel, while it is also clear that considerable problems may appear shortly after excavation of tunnels in relatively richly fractured rock.

Taking the structure of the tunnel roof in Fig.13 as an example, successive disintegration is initiated when the most critically located and stressed block has moved sufficiently much relatively to the adjacent ones to offer less effective support to them. The movement of the blocks is due to creep and if the rate of creep rate can be reasonably well estimated one can also predict the process of roof disintegration, provided that the block structure geometry can be defined. Following the same reasoning as for the deposition holes, but assuming a critical strain of about 10^{-3} for reduction of the peak shear strength to the residual strength, and considering that the creep rate is probably higher due to the high content of induced fractures and fissures - a value of 10^{-3} for each decade of seconds would be realistic - we would arrive at the same degradation rate as for the deposition holes. Thus, it is estimated that significant strength reduction occurs in a few hundred years in the blast-disturbed zone, resulting in unstable conditions and risk of rock fall.

Retardation of the degradation processes would require very substantial external supporting pressure supplied by the tunnel backfill, i.e. to approximately the same values as the tangential stress, which is several MPa. Moderation of the fracture expansion would in fact also require a high supporting pressure, while prevention of rock fall would only require about 50 kPa, which is offered by a 20/80 bentonite/sand backfill with a density at saturation of 1.9 g/cm^3. In practice, the disturbed zone which is primarily developed in the roof but which is also formed in the upper part of the walls, will serve as water conductor in a repository with an axial hydraulic conductivity that may initially not be very much higher than that of the virgin rock, but that may increase strongly in the course of time.

As indicated by the colored pictures in Fig.14 the rock located over the disturbed zone will be exposed to high stresses, leading to creep-induced strain and drop in strength also above the zone of disturbance. Here, the conditions will be similar to those in the rock surrounding the deposition holes, which means that although there will be a strain-induced drop in strength, the stability will not be endangered except in the presence of rock wedges. Still, the hydraulic conductivity will increase somewhat also up to approximately 1 m height over the blast-disturbed zone. Together, the two zones combine to yield a continuous conductive passage along the tunnels.

6 NUMERICAL CALCULATIONS

6.1 OBJECTIVES

The objective of the study presented here was to examine the possibility of performing numerical simulations involving rock that exhibits time dependent material behavior by applying a simple creep model to the rock surrounding a circular opening in a biaxial stress field. It should be investigated if the response of the numerical model was logical, i.e. physically explainable, and of correct order of magnitude considering the numerical input. It should also be investigated if calculations with realistic input data could be performed within reasonable execution times.

6.2 NUMERICAL MODELING METHOD

The calculation presented in this chapter was performed using version 3.2 of the two-dimensional finite difference code FLAC (Fast Lagrangian Analysis of Continua). FLAC is a recognized tool for analyzing rock- and soil hydromechanical, thermomechanical or purely mechanical problems (20). The problem domain is discretized into a mesh of quadrilateral zones with gridpoints in the zone corners. A number of material models are available, including creep models. Different material models may be assigned to different parts of the calculation grid or to individual zones.

FLAC contains a built-in programming language, 'FISH', which enables the user to define new variables and functions (20). The FISH language can, for instance, be used to write functions that automatically creates grids of specific shapes, or functions that automatically distribute material models or material properties in specific user-defined patterns. It is also possible to define extra gridpoint variables (for instance for printing or plotting purposes) by use of FISH functions. FISH can be used to modify existing material models or even to specify new ones.

6.3 MODEL DESCRIPTION

6.3.1 Problem Geometry

The shape of the excavation was circular with a diameter of 2.4 m. The distance from the excavation center to the model boundary was 25 m. A 0.5 m deep region around the periphery was assumed to exhibit creep behavior while the rock outside this region was assumed to be purely elastic. Fig.16 shows the grid

and Fig.17 shows a close-up view of the tunnel region. The grid was generated using a FISH routine, contained in the FISH routine library supplied with the FLAC code, which automatically maps gridpoints to a quarter symmetry donut-shaped mesh with user-specified inner and outer diameters and with continuously increasing distances between circular gridlines. The FISH routine was modified for this model to give equal distances between circular gridlines within the creep region and to make the areas of zones located adjacent to the vertical and horizontal boundaries half the areas of zones in the inner part in order to reproduce true symmetry about the coordinate axes.

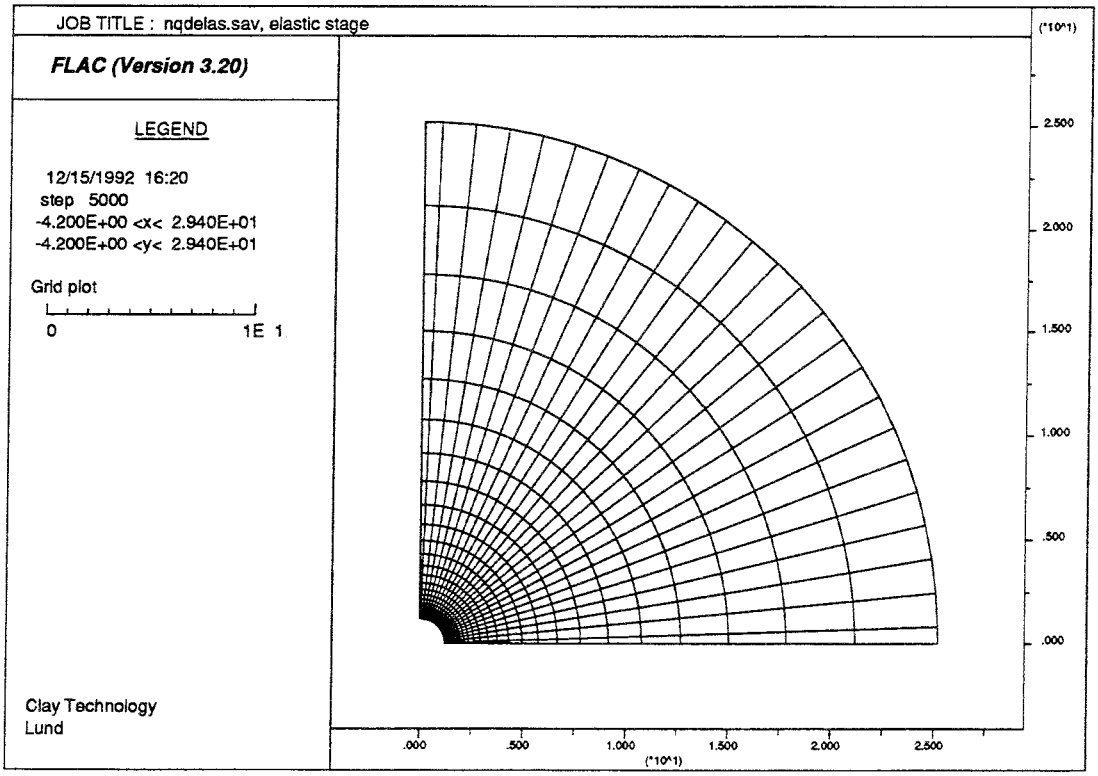

Figure 16 FLAC grid

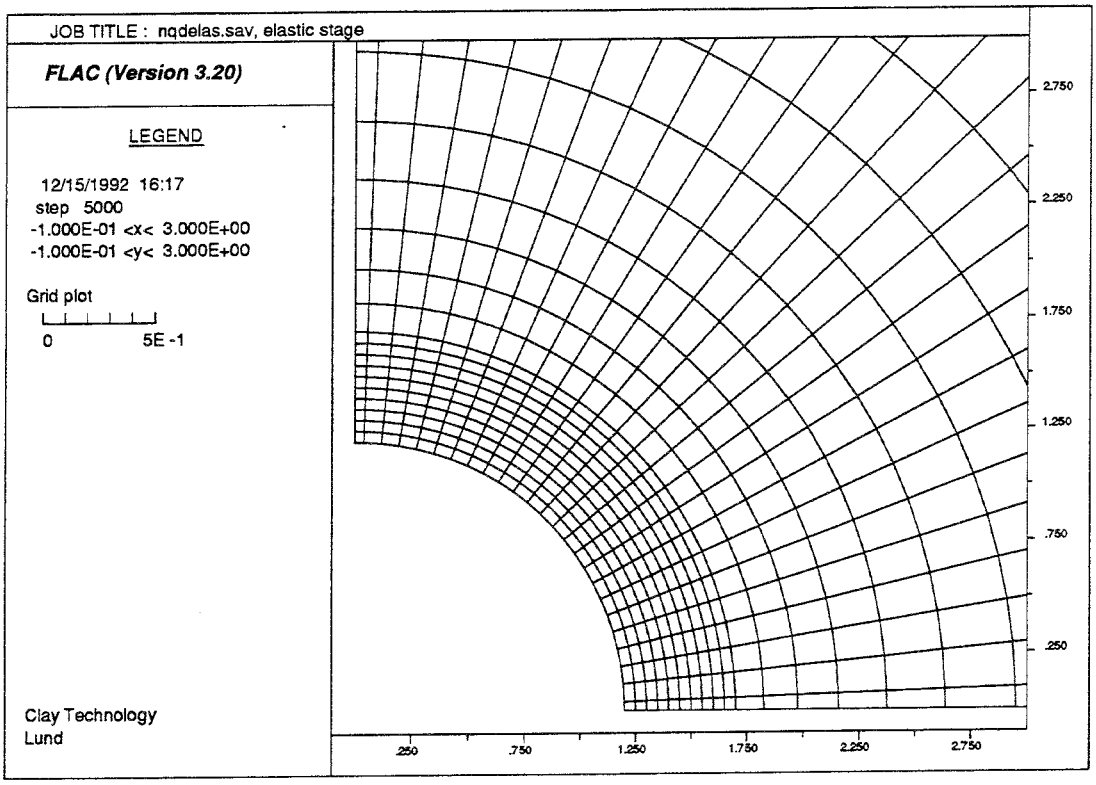

Figure 17 Close-up view of tunnel region

6.3.2 Creep Law

The material in the 0.5 m deep zone was described by Kelvin type rheological elements. A Kelvin element corresponds to an elastic spring and a dashpot, i.e. a purely viscous element, in parallel. The strain vs time relation for a Kelvin material under constant stress is given by Eq.(18) below.

$$\varepsilon = \frac{\sigma}{k} \left(1 - \exp(-\frac{k}{\eta} \cdot t) \right) \qquad (18)$$

Where
ε = strain
σ = stress
k = elasticity constant
η = viscosity
t = time

There is no built-in Kelvin model in FLAC, but the effects of a Kelvin material may be obtained by mixing elastic and viscous zones as shown in Fig.18. This distribution of material models was accomplished by writing and executing a FISH function. The FLAC material model assigned to the viscous zones are of Maxwell type, i.e. may be represented by an elastic spring and a dashpot in series.

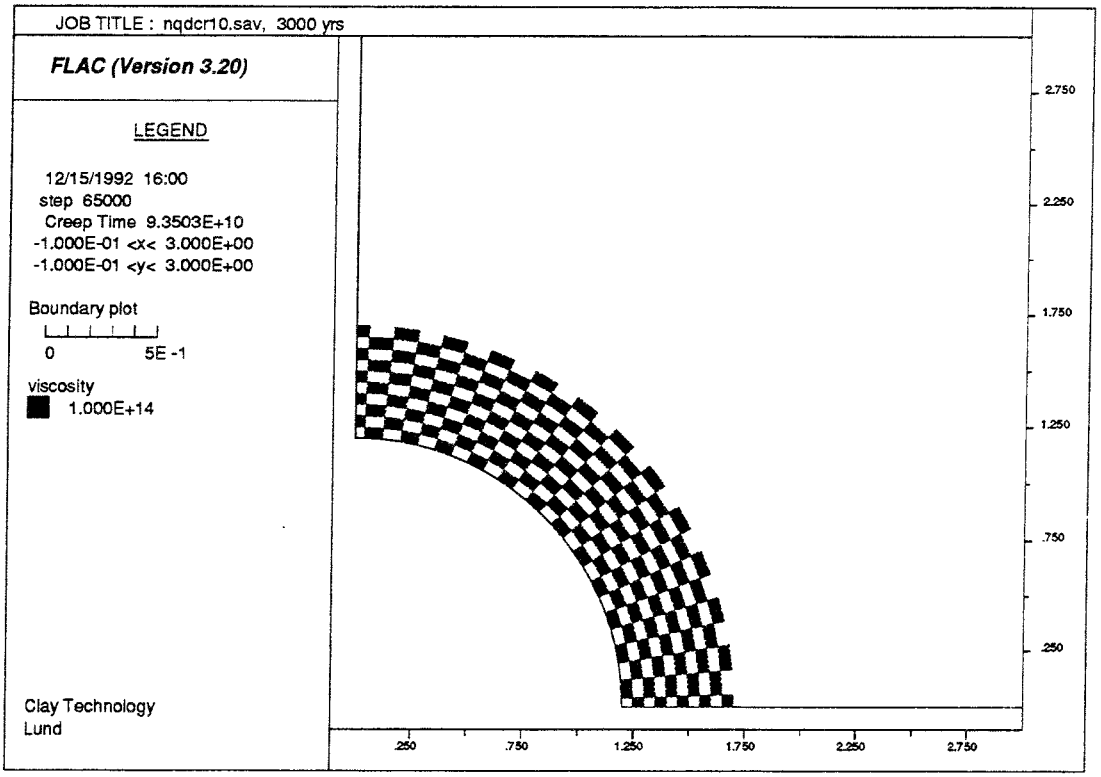

Figure 18 Checkboard pattern of alternating viscous and elastic zones

The discussion in preceding chapters concerns log-time creep laws of the form

$$\varepsilon = A \cdot \ln(t + t_o). \qquad (19)$$

where

ε = strain,

A = dimensionless constant related to stress and temperature,

t = time,

t_o = constant which is significant only in the beginning of the creep process.

FLAC does not contain logtime creep laws. In this study a Kelvin model was used to approximate logtime behavior. Fig.19 shows a comparison of creep curves obtained using the Eqs. (18) and (19). The parameter values used to generate these curves are given in Table 3.

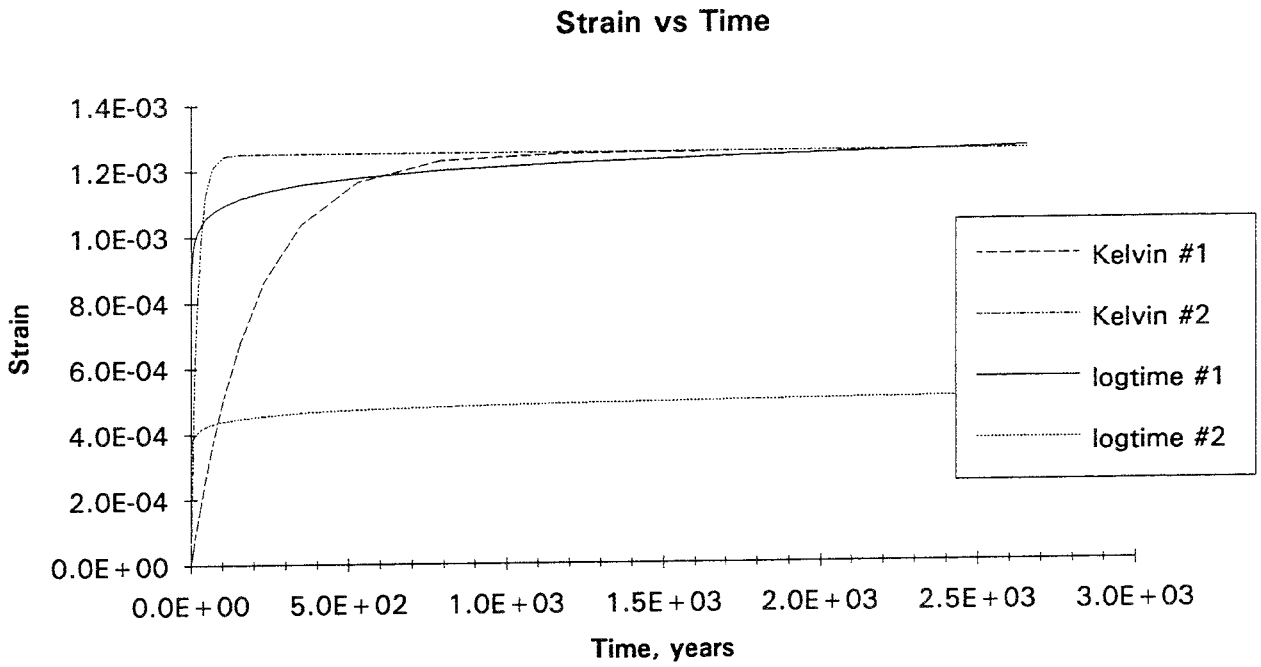

Figure 19 Kelvin and logtime creep curves

Table 3: Parameter values for theoretical creep curves

Kelvin Accord. to Eq.(18)		*logtime Accord. to Eq.(19)*	
#1	σ = 20 MPa	#1	A = $5*10^{-5}$
	k = $16*10^{3}$ MPa		t_o = 0 s
	η = $1*10^{14}$ MPas		
#2	σ = 20 MPa	#2	A = $2*10^{-5}$
	k = $16*10^{3}$ MPa		t_o = 0 s
	η = $1*10^{12}$ MPas		

The curves representing Kelvin materials differ only in viscosity. Note that the viscosity, according to Eq.(18), affects only the time scale of the creep process, whereas the final total displacement depends on the stress level and on the elastic constant.

The creep curves given in previous chapters (Figs. 2, 8 and 9) represent logtime creep processes in samples subjected to high uniaxial compression. The constant 'A' in Eq. (19), as derived from these curves, appears to equal approximately 1E-4.

6.3.3 Material Properties and In-Situ Conditions

Parameter values for the material properties are given below:

Bulk modulus	22 GPa
Shear modulus	16 GPa
Viscosity	10^{14} MPas
	(= 10^{21}Pois, viscous zones only)

The primary stresses were:

σ_h = 25 MPa

σ_v = 10 MPa

Roller boundaries were applied to the symmetry axes while zero velocity was prescribed for the other boundaries.

6.4 MODELING PROCEDURE

6.4.1 Elastic Phase

The excavation was simulated by removing the fixed conditions for gridpoints at the tunnel periphery. The number of calculation steps, necessary to achieve a new state of equilibrium, was performed without invoking the creep logic, i.e. under purely elastic conditions.

6.4.2. Creep Phase

The state of mechanical equilibrium achieved during the elastic phase was used as point of departure for the subsequent creep simulation. The creep logic was put in operation beginning with very small timesteps and taking successively larger timesteps as the driving forces, i.e. shear stresses in the viscous zones, were getting smaller. The creep process was simulated for a period of 3000 years. For a Kelvin material with elastic constant = 16 MPa (shear modulus in the model) and viscosity = 1E+14 MPas, about 90 percent of the final deformation will develop within 500 years, meaning that at the end of the simulation all shear stresses in the viscous zones should be approximately zero.

6.5 RESULTS

6.5.1 Elastic Phase

Fig.20 shows initial elastic displacements caused by the excavation. The results agree well with analytical expressions for displacements around a circular opening in an infinite elastic medium with the primary stresses assumed here (20). The maximum inward displacement of the periphery takes place in the springline and amounts to 1.25 mm.

Fig.21 shows contours of maximum principal stresses. Also the stress field is in agreement with analytical expression. The maximum stress is found in the crown and amounts to about 65 MPa. Fig.22 shows contours of deviator stresses.

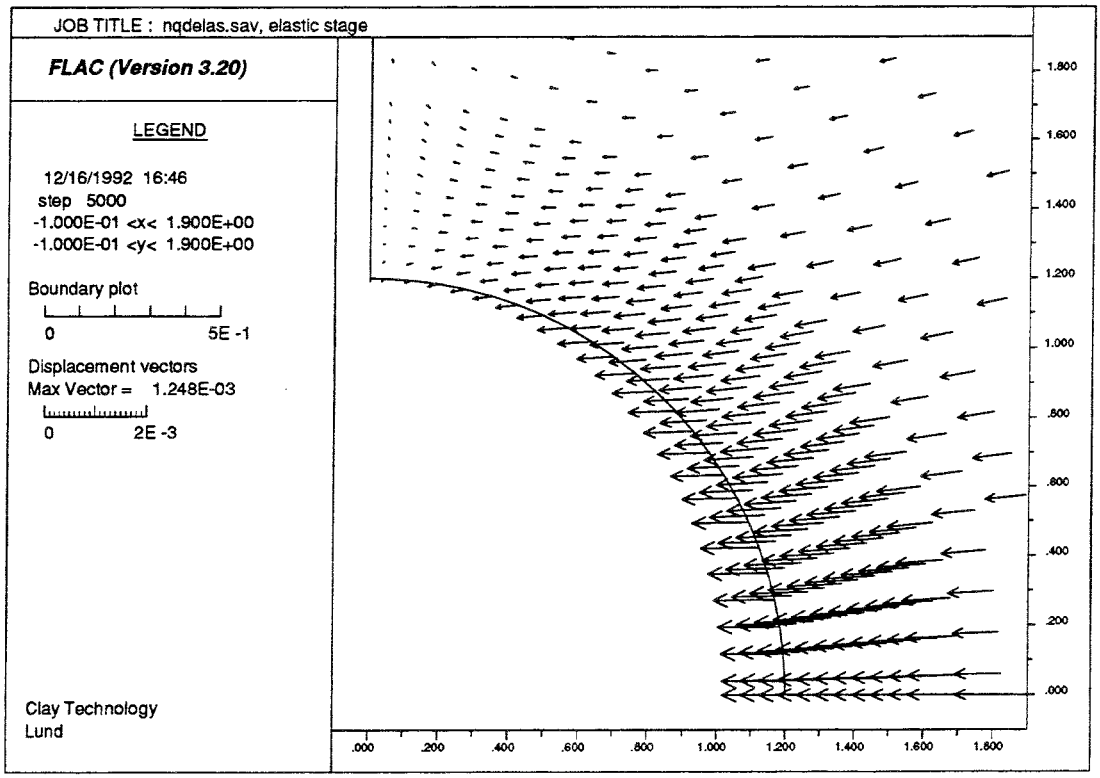

Figure 20 Initial elastic displacements. Max displ. = 1.25 mm

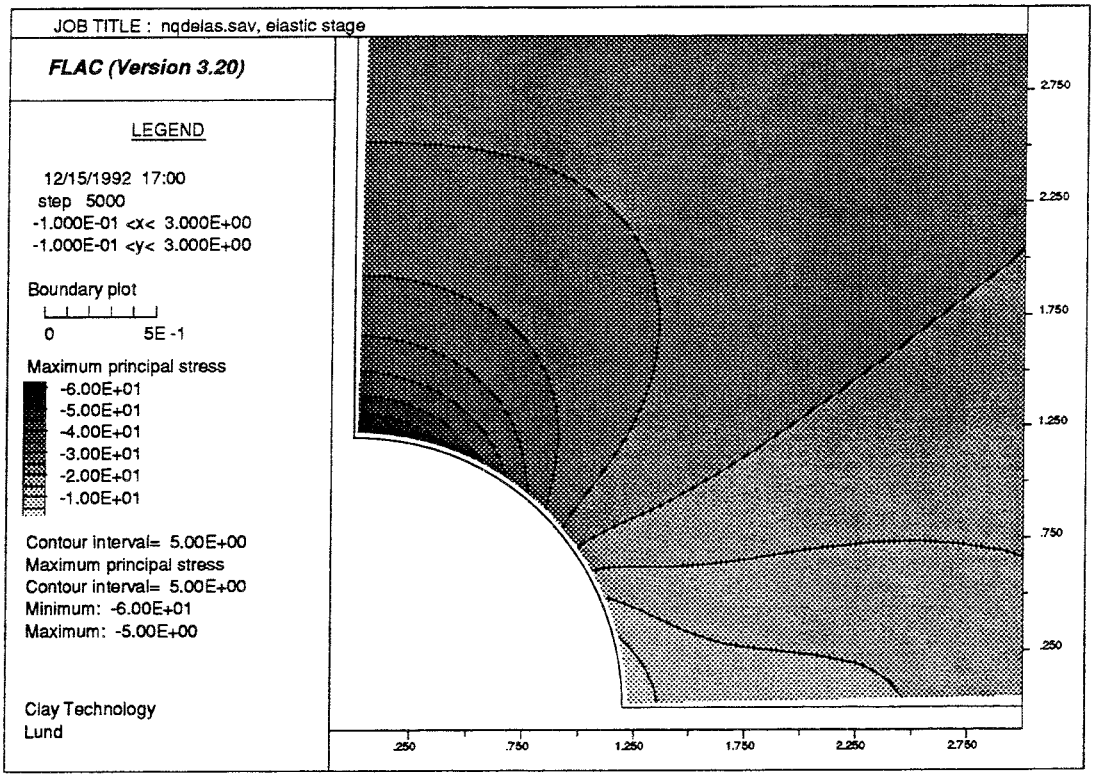

Figure 21 Major principal stress contours, elastic stage

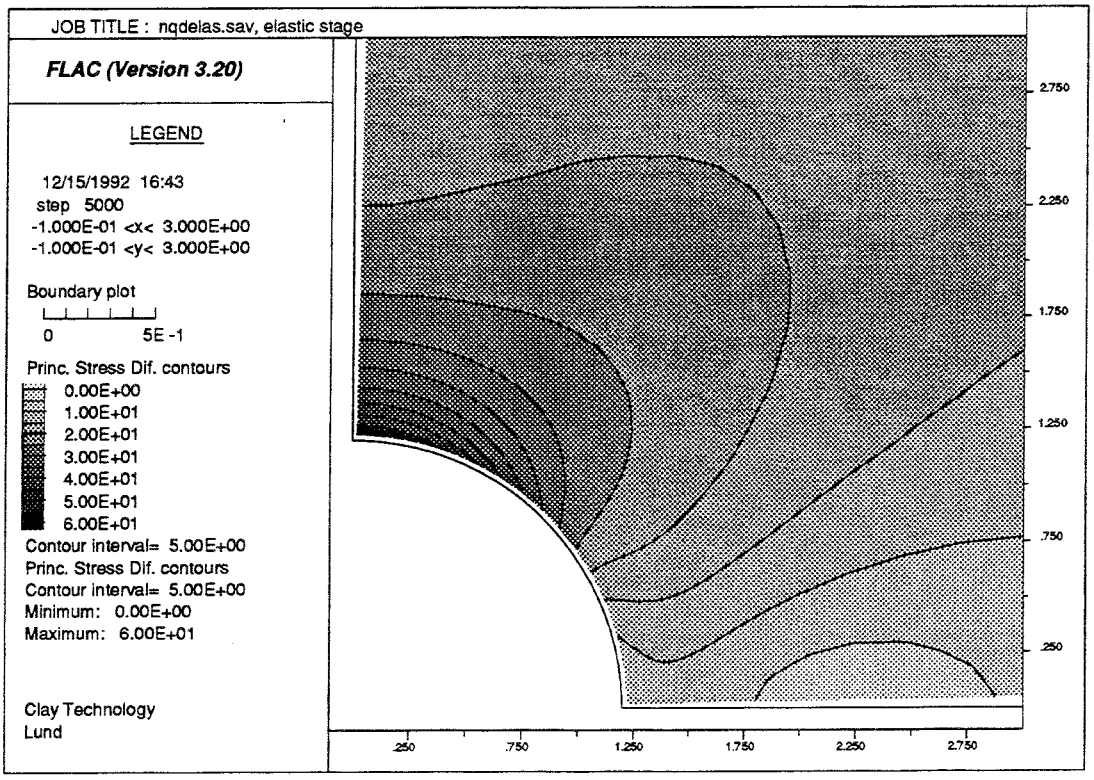

Figure 22 Principal stress difference contours, elastic stage

6.5.2 Creep Phase

6.5.2.1 Deformations

Fig.23 shows displacements accumulated during the 3000 years of creep deformation that were simulated. The initial displacements obtained in the elastic stage are not included.

Fig.24 shows the inward displacement in the crown and in the springline as function of creep time. The small figure in the upper right part shows this process in detail for the first 250 years. Creep time is in seconds. According to Eq.(18), 50 percent of the final displacement should develop within 43E+8 seconds for a Kelvin material with the values for shear modulus and viscosity assumed in the FLAC calculation. From Fig.24 it appears that 50 percent was reached after about 70E+8 seconds in the FLAC model, with a time delay of about 60 % compared to the theoretical Kelvin process. Expression (18), however, is an idealization of a one-dimensional constant stress deformation. Considering this the checkboard representation of the Kelvin material performs adequately with respect to timescale.

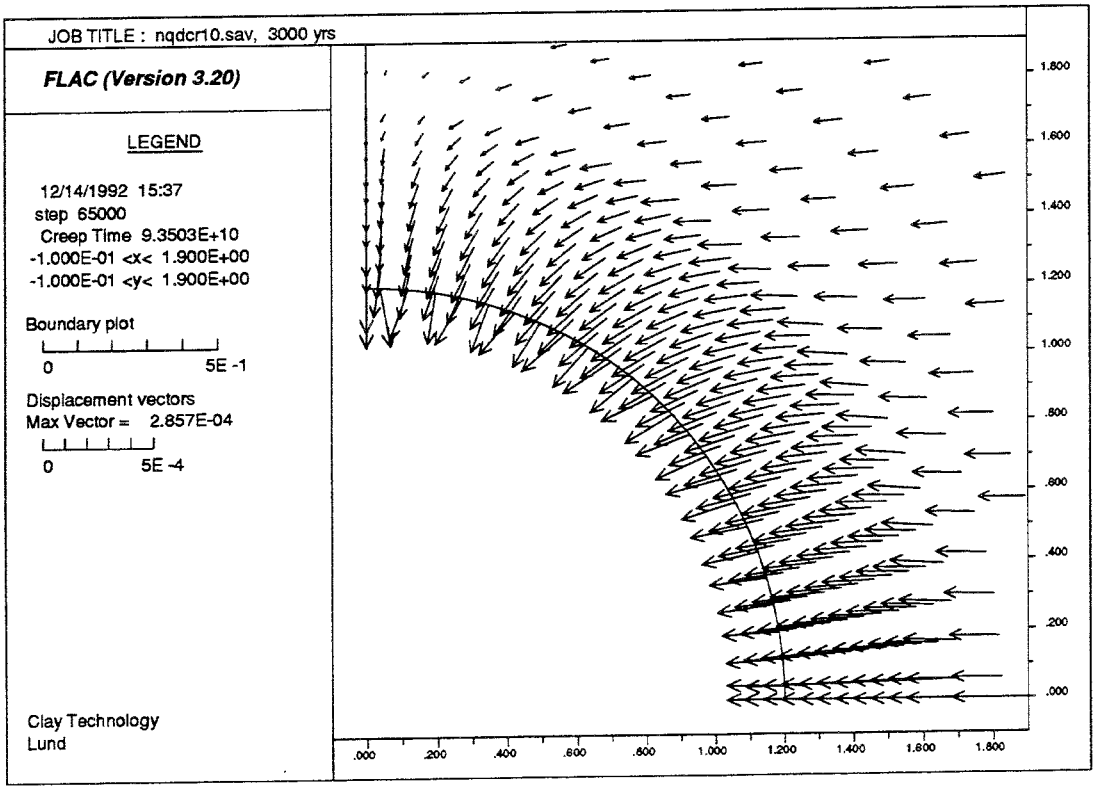

Figure 23 Creep deformations after 3000 years. Maximum displacement is about 300 μm

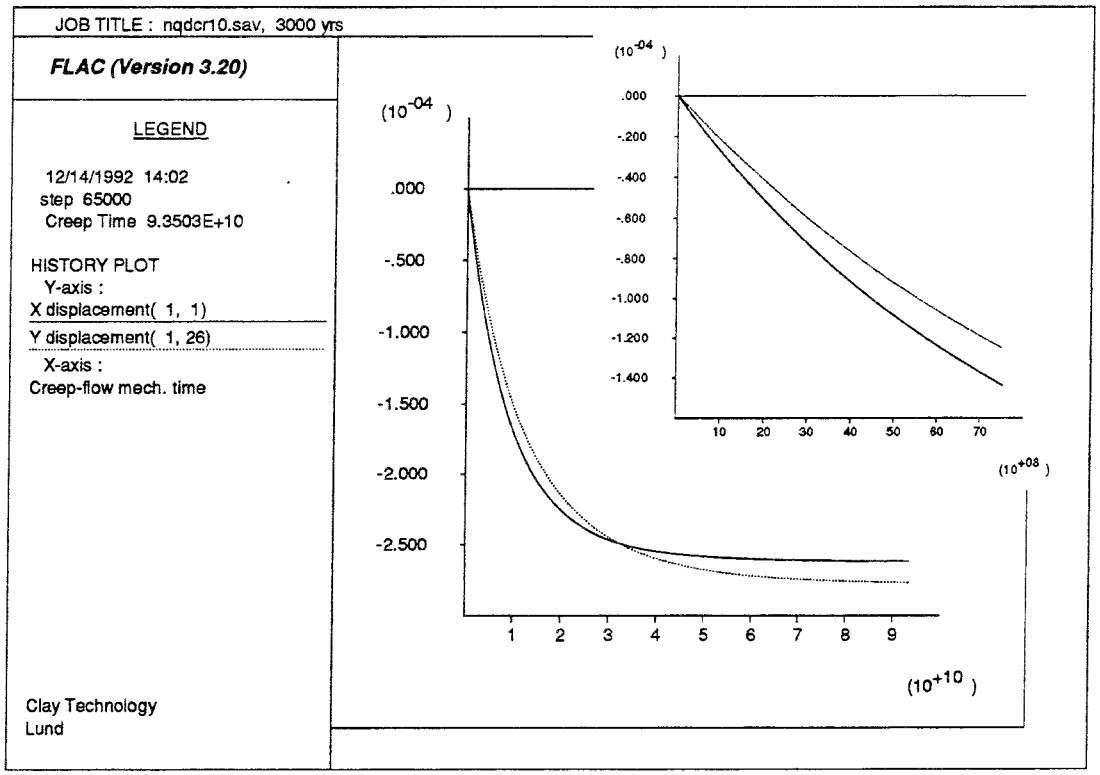

Figure 24 Time-dependent radial displacements in meters at the periphery. Solid line is springline, dotted line crown. The small figure in the upper right part shows first 250 years. Horizontal axis is in m, vertical axis in seconds

Fig.25 shows the radial expansion of the creep zone after 250 years and Fig.26 shows the final radial expansion, i.e. after 3000 years. The contours denote radial displacements relative to the outer boundary of the 0.5 m deep creep zone. The maximum expansion takes place in the crown and amounts to 100 μm after 250 years and 225 μm after 3000 years. Corresponding values for the springline are 10 μm and 25 μm, respectively. Final radial strains are thus:

$$\varepsilon_{crown} = 2.25*10^{-4}/0.5 = 4.5*10^{-4}$$

$$\varepsilon_{springline} = 2.5*10^{-5}/0.5 = 5.0*10^{-5}$$

For a stress of 20 MPa (= approximately the shear stress in the roof region after excavation) and an elasticity constant of 16E+3 MPa (= shear modulus in the FLAC model), Eq(18) gives a final strain of 1.25E-3, i.e. between twice and three times the value found in the model. With respect to order of magnitude this is within reasonable agreement, considering that the stress in Eq.(18) is assumed to be constant, whereas the stress in the FLAC model decreased with time.

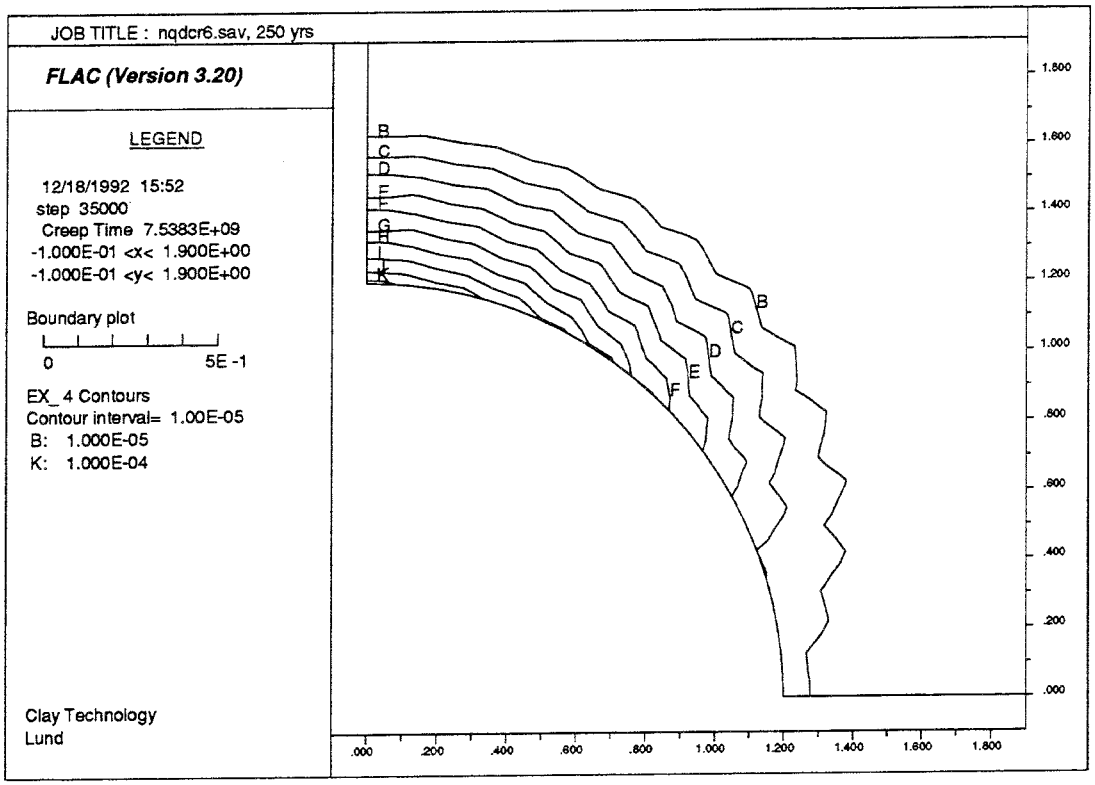

Figure 25 Radial expansion of creep region after 250 years. Contour lines B and K correspond to 10 μm and 100 μm, respectively

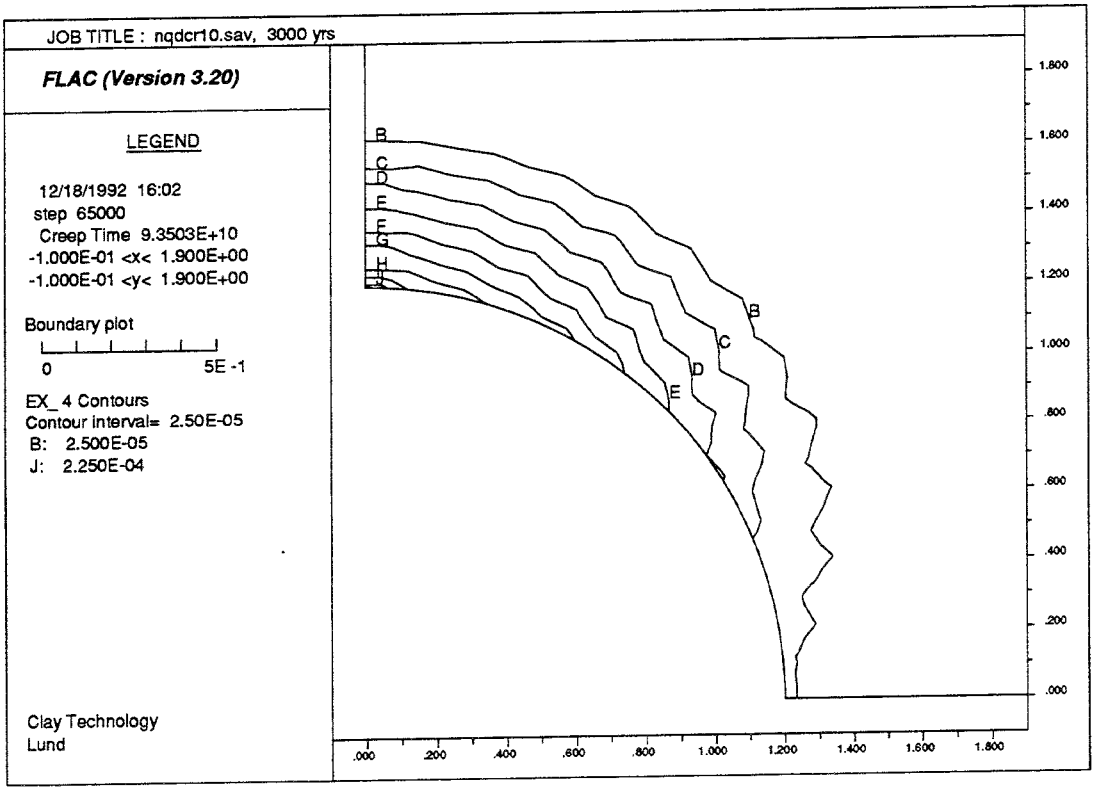

Figure 26 Radial expansion of creep region after 3000 years. Contour lines B and K correspond to 25 μm and 250 μm, respectively

6.5.2.2 Stresses

Fig.27 shows principal stresses, obtained in FLAC model, vs creep time for two neighboring zones (i.e. one elastic and the other viscous) located between crown and springline at the periphery of the tunnel. Vertical axis is in MPa, negative numbers denoting compression. The horizontal axis is in seconds. At the beginning of the creep process, i.e. in the state of elastic equilibrium described above, the minor stresses (radial) in both zones are zero, while the major stresses (tangential) are 30 MPa and 34 MPa. This gives an average deviator stress of 32 MPa for the two zones. The average major principal stress is also 32 MPa. As creep progresses both principal stresses in the viscous zone approach 13 MPa, giving zero deviator stress. In the elastic zone the principal stresses approach 14 MPa (tension) and 30 MPa (compression), giving a deviator stress of 44 MPa. This means that the average major principal stress for the two zones at the end of the creep process was (30+13)/2 = 21.5 MPa and that the average deviator stress was (44+0)/2 = 22 MPa. The transfer of shear stresses from viscous zones to elastic zones is characteristic for a Kelvin material. The reduction in average stress level depends on the nature of the

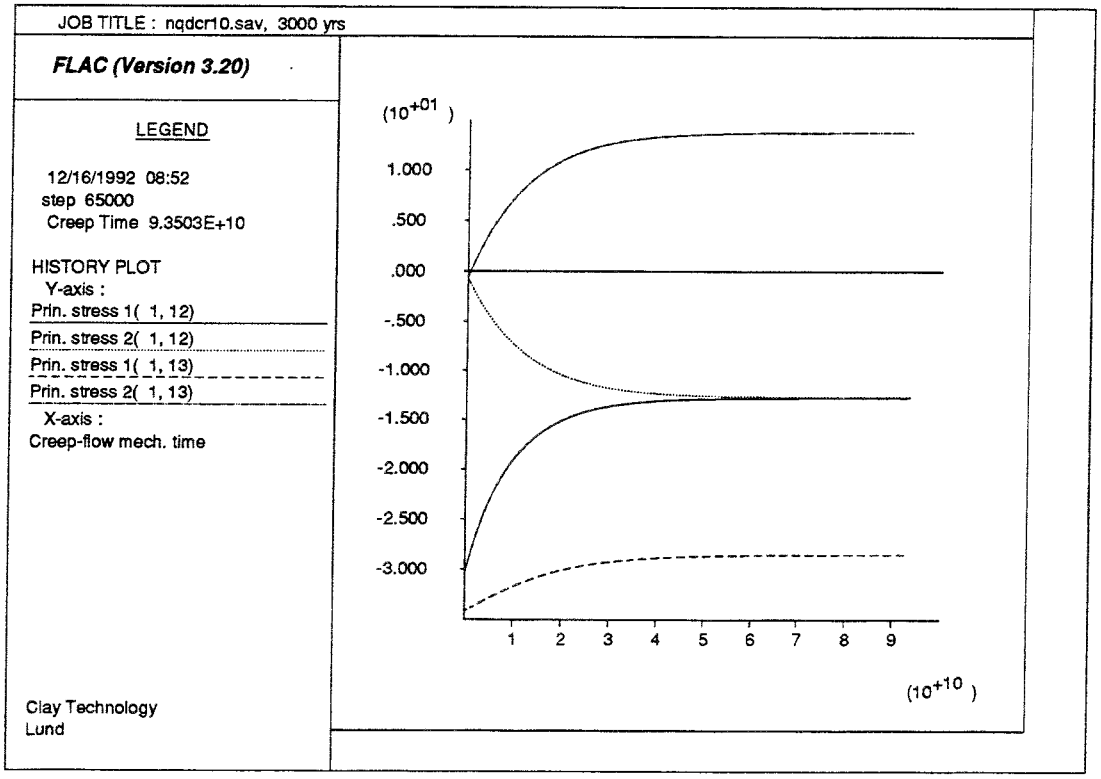

Figure 27 Principal stresses in neighboring periphery zones vs time. Upper and lower curves: elastic zone. Middle curves: viscous zone. Horizontal axis is in seconds, vertical axis is in MPa

problem, i.e. the stresses applied to the Kelvin material were reduced with time as a result of the inward displacement of the tunnel periphery.

Fig.28 shows major principal stress contours in the roof region after 3000 years and illustrates how stresses are transferred from viscous components to elastic components in the creep process.

A FISH function, which computes the principal stresses and the deviator stress in each individual gridpoint by taking the average of corresponding stresses in the four zones neighboring the gridpoint, was designed and executed to give a better picture of the stress field. Periphery gridpoints have only two neighboring zones, which means that the stress at the periphery will be slightly underestimated. Fig.29 shows major principal stress contours after 3000 years, plotted using the average stress FISH function. Fig.30 shows corresponding deviator stress contours. The stress reduction in the creep region is illustrated by both plots. There is also a small raise in stress level immediately outside the creep region. This is illustrated also by Fig.31, which shows the major principal stress in gridpoints on the vertical symmetry line, i.e. the tangential stress above the roof. The gridpoint stresses were computed by use of the average stress FISH function for the elastic equilibrium state and for the state after 3000 years of creep deformation.

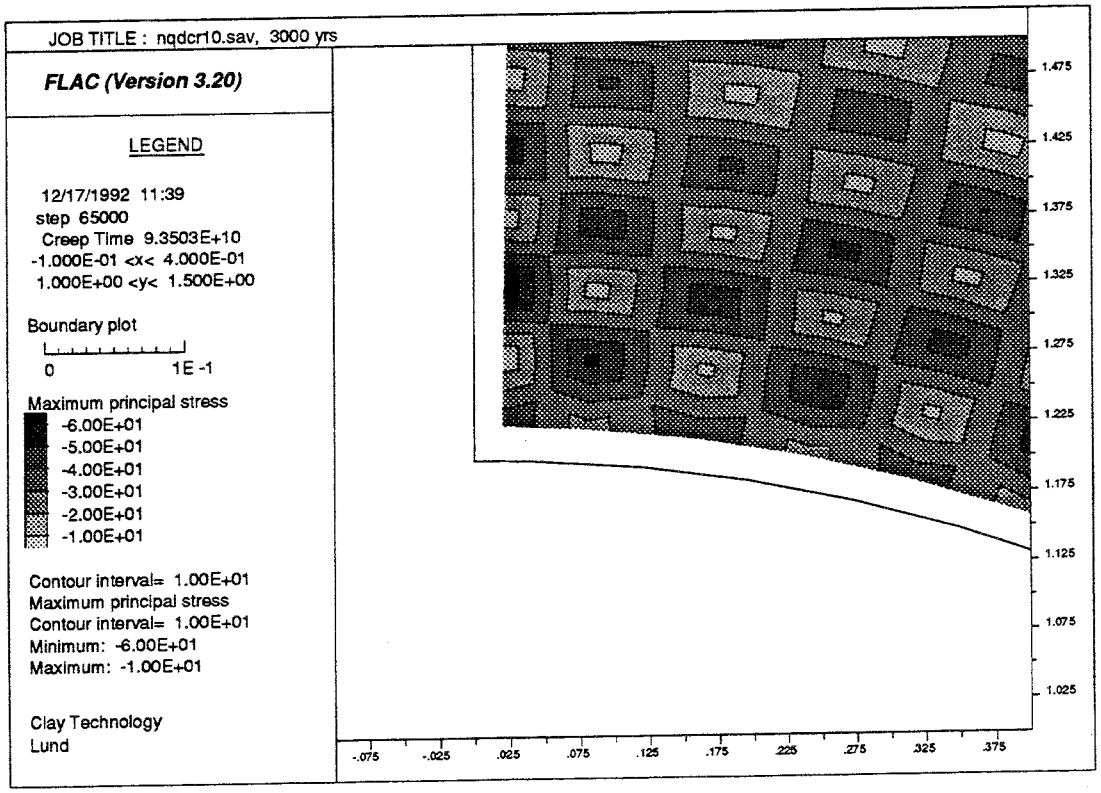

Figure 28 Major principal stress contours in MPa in roof region

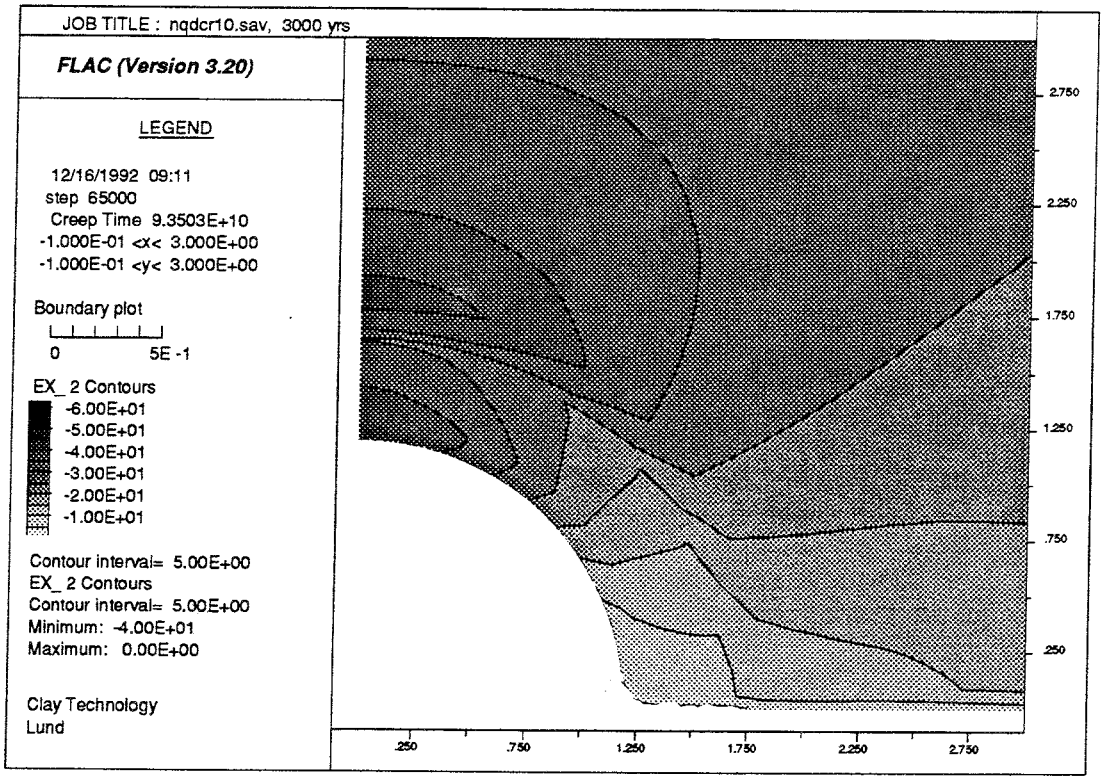

Figure 29 Major principal stress contours (MPa) after 3000 years. Stresses computed using FISH average stress function.

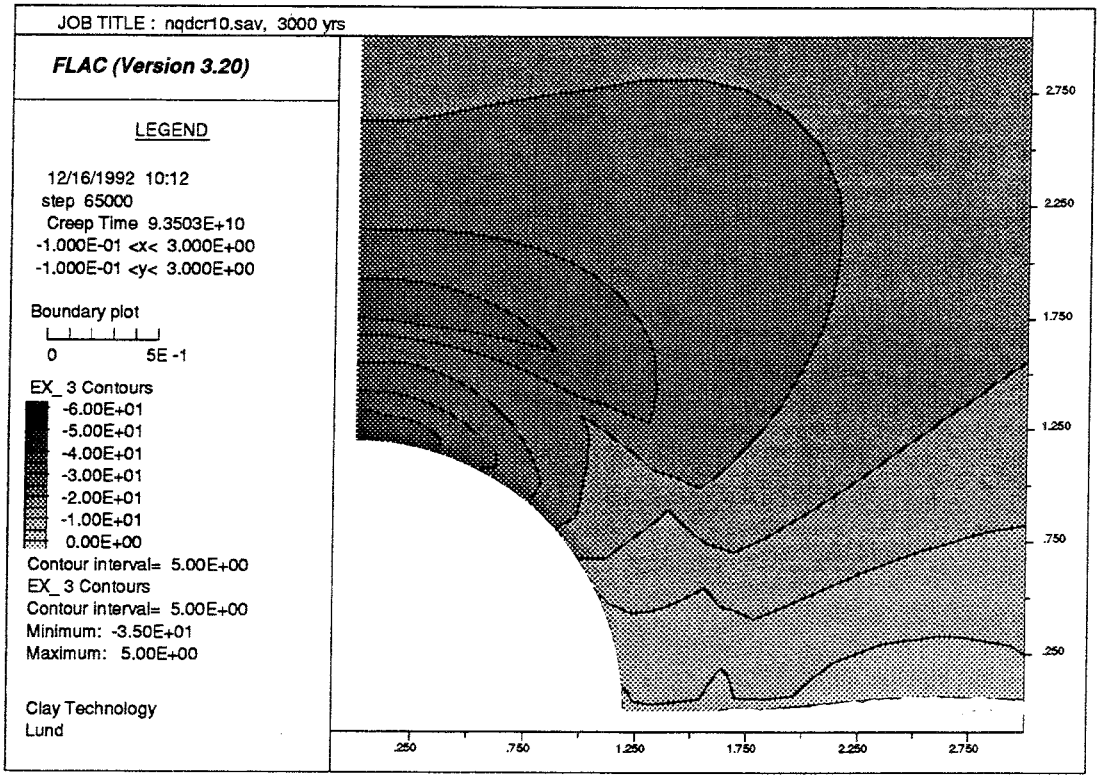

Figure 30 Deviator stress contours (MPa) after 3000 years. Stresses computed using FISH average stress function

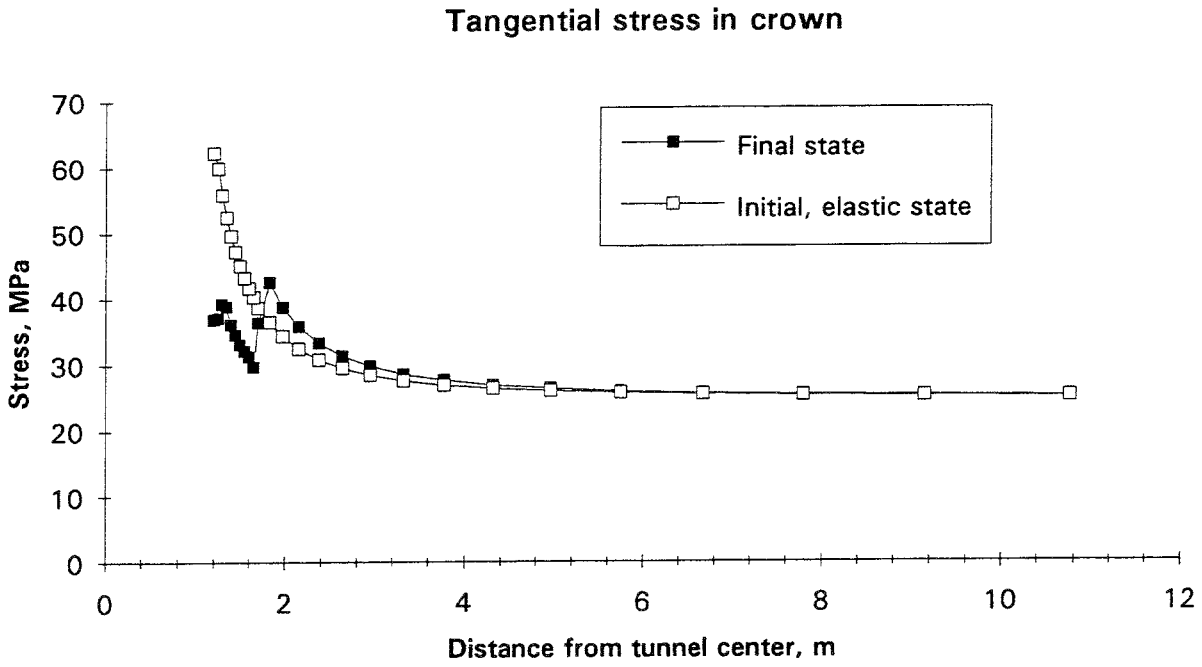

Figure 31 Tangential stresses above the roof. Stresses calculated using FISH average stress function

6.6 DISCUSSION

The model studied here is not intended as a prediction or as a description of true time dependent deformation characteristics for rock surrounding tunnels. The use of a Kelvin rheological model may be a too simple approach, keeping in mind the commonly observed logtime creep, and the geometrical distribution of viscous zones was very schematic. Although it is probable that creep should be primarily associated with rock that has been disturbed or damaged by excavation, which implies activation of the hierarchy of finer discontinuities (5th - 7th order) and formation of new ones, other conditions, related to basic structural inhomogeneities, like the natural discontinuities of long extension, termed 4th order breaks, may be important as well. Thus, their extension and low strength mean that they control the strain in virgin rock and naturally contribute to the gross creep also in the disturbed zone. Their contribution naturally depends on their frequency and orientation with respect to the local stress field.

The study shows, however, that time-dependent processes can be simulated in a physically meaningful way for media that can be approximated by continuum models.

The following items were not covered by this study:

- Shear failure due to limited strength of non-viscous zones. This could be modeled by substituting Mohr-Coulomb Zones for the purely elastic zones in the creep region.

- Other geometrical assumptions regarding the extension of region exhibiting creep behavior.

- Other time dependent material models contained in FLAC, e.g. Norton Power law relation.

- Improved approximation to logtime creep by other combinations of material models or by modification of existing material models

7 CONCLUSIONS

7.1 PRACTICAL IMPORTANCE OF CREEP STRAIN

Assuming that strain is uniquely related to strength and that significant strength reduction is associated with a critical strain irrespective of whether it is produced by short- or long-term loading, it is estimated that creep-induced strain taking place in the rock surrounding deposition holes does not yield failure even in a very long time perspective.

For KBS3 tunnel roofs the situation is probably different because the degradation and expansion yielding significant loss in strength leads to more shear strain than evaluated from the numerical calculations. Potential lack of stability is therefore expected in a few hundred years in the blast-disturbed zone. Above this zone the virtually intact rock is exposed to high stresses and will undergo creep without leading to failure but implying some increase in hydraulic conductivity.

The support pressure provided by the backfill will not alter the elastic stress distribution around the tunnel significantly. For the example investigated in the FLAC calculation preliminary calculations show that a pressure of 10 MPa, applied to the tunnel walls, would be necessary to reduce the time dependent inward displacement by 50 %. This example considered a case in which stress transfer from viscous to non-viscous components did not result in failure. More realistic cases would include the possibility of failure, which would give larger inward displacements. In such cases the function of the backfill is to maintain the frictional interaction between slipping rock blocks, which requires much smaller backfill pressures.

8 REFERENCES

1. Pusch,R. Mechanisms and Consequences of Creep in Crystalline Rock. Comprehensive Rock Engineering. Pergamon Press, 1992

2. Matsushima, S. On the Flow and Fracture of Igneous Rock. Disaster Prevention Res. Institute. Bull. No. 36, Kyoto, 1960.

3. Murrel, S.A.F. & Misra, A.K. Time-dependent Strain or "Creep" in Rocks and Similar Nonmetallic Materials. Trans. Inst. Min. Metall. Vol. 71, 1962 (pp 353-378)

4. Rummel, F. Studies of Time-dependent Deformation of Some Granite and Eclogite Rock Samples under Uniaxial, Constant Compressive Stress and Temperatures up to 400°C. Zeitschr. für Geophysik, Band 35, 1969 (pp. 17-42)

5. Dorn, J.E. Some Fundamental Experiments on High-temperature Creep. J. Mech. Phys. Solids, Vol. 19, 1954 (pp. 77-83)

6. Carter, N.L. & Kirby, S.H. Transient Creep and Semibrittle Behavior of Crystalline Rocks. Pure and Applied Geophysics. Vol. 116, Nos. 4/5, 1978 (pp. 807-839)

7. Pusch, R. Creep Mechanisms in Clay. Proc. Inter-disciplinary Conference on Mechanisms of Deformation and Fracture, University of Luleå (Sweden) 1978, Vol. 1.

8. Feltham, P. A Simple Stochastic Model of Low-temperature Creep and Stress-relaxation in Solids. Proc. VIIth Int. Congr. Rheology, Gothenburg, Sweden 1976 (pp. 166-167).

9. Weertman, J. Creep Laws for the Mantle of the Earth. Phil. Trans. R. Soc. Lond. A. Vol. 288, 1978 (pp. 9-26).

10. Börgesson, L. Stripa Project - Final Report of the Rock Sealing Project. Volume I: Sealing of the Near-field Rock around Deposition Holes, Swedish Nuclear Fuel Waste Management, Stockholm, 1991

11. Rahm,L. Deformations- och ljudhastighetsmätningar i bergtunnlar. Bergmekanik, Ingenjörsvetenskapsakademins Meddelande 142, Stockholm, 1965

12. Pusch, R. Bearing Capacity and Settlement at High Loads on Rock (In Swedish). Report no 11, Svenska Byggnadsentreprenörföreningen, 1974

13. Skaanes, S. Mechanisches Tunnelausbruch am Beispiel Baulos Huttegg des Seeligbergtunnels. Proc. Int. Congr. Rock Mechanics, 4th, Montreux, 1979, Vol.1 (pp.551-556)

14. Thomson, S., and El-Nahhas, F. Field Measurements in Two Tunnels in Edmonton, Alberta. Can. Geotech. J., 17(1), 1980 (pp.20-33)

15. Pusch,R. SFR-Buffertar, Alternativ Med Bentonit/ Sandfyllning. SFR Slutförvar för Reaktoravfall. SKBF/KBS Teknisk Rapport SFR 81-06, 1981

16. Pusch, R. and Hökmark, H. Characterization of Structure and Stress State of Nearfield Rock with Respect to the Influence of Blasting. Proc. Conf. FRAGBLAST-4, Vienna, July 1993 (in press)

17. Atkinson, B.K. A Fracture Mechanics Study of Subcritical Tensile Cracking of Quartz in Wet Environment. Pageoph, No. 117, 1980 (pp. 1011-1024).

18. Kuhnel, R.A. and Van der Gaast, S.J. Formation of Clay Minerals by Mechanochemical Reactions During Grinding of Basalt under Water. Appl. Clay Sci., Vol.4, 1989

19. Carter, N.L., Anderson, D.A., Hansen, F.D. and Krantz. R.L. Creep and Creep Rupture of Granitic Rocks. Mechanical Behaviour of Crustal Rocks. Geophysical Monograph 24, Am. Geophys. Union, 1981.

20. Pusch,R. and Hökmark,H. Characterization of Nearfield Rock - A Basis for Comparison of Repository Concepts. SKB Technical Report 92-06, 1992

21. FLAC Fast Lagrangian Analysis of Continua. Ver 3.2. Manual. Itasca Consulting Group, Inc. Minneapolis 1992

22. Brady,B.H.G. and Brown,E.T. Rock Mechanics for Underground Mining. Allen & Unwin, London 1985

9 LEGEND

$\propto$ = proportionality symbol

α, β = coefficients
ε = strain
$\dot{\varepsilon}$ = strain rate (s^{-1})
σ = normal stress (MPa)
τ = shear stress (MPa)
$f(\sigma)$ = stress function
ν = vibrational frequency (s^{-1})
ϕ = function of u, t and T
η = viscosity (Pas)

k = Boltzmann's constant, also elasticity constant
n = function of distribution of u and t
r = function of n and T
t = time (s)
t_o = integration constant (s)
u = creep activation energy (eV, kcal/mole)

A = coefficient
D = function of u and T
E = modulus of elasticity (MPa, GPa)
N = probability function
R = universal gas constant
T = temperature (°C, K)
V = volume (m^3)

List of SKB reports

Annual Reports

1977-78
TR 121
KBS Technical Reports 1 – 120
Summaries
Stockholm, May 1979

1979
TR 79-28
The KBS Annual Report 1979
KBS Technical Reports 79-01 – 79-27
Summaries
Stockholm, March 1980

1980
TR 80-26
The KBS Annual Report 1980
KBS Technical Reports 80-01 – 80-25
Summaries
Stockholm, March 1981

1981
TR 81-17
The KBS Annual Report 1981
KBS Technical Reports 81-01 – 81-16
Summaries
Stockholm, April 1982

1982
TR 82-28
The KBS Annual Report 1982
KBS Technical Reports 82-01 – 82-27
Summaries
Stockholm, July 1983

1983
TR 83-77
The KBS Annual Report 1983
KBS Technical Reports 83-01 – 83-76
Summaries
Stockholm, June 1984

1984
TR 85-01
Annual Research and Development Report 1984
Including Summaries of Technical Reports Issued during 1984. (Technical Reports 84-01 – 84-19)
Stockholm, June 1985

1985
TR 85-20
Annual Research and Development Report 1985
Including Summaries of Technical Reports Issued during 1985. (Technical Reports 85-01 – 85-19)
Stockholm, May 1986

1986
TR 86-31
SKB Annual Report 1986
Including Summaries of Technical Reports Issued during 1986
Stockholm, May 1987

1987
TR 87-33
SKB Annual Report 1987
Including Summaries of Technical Reports Issued during 1987
Stockholm, May 1988

1988
TR 88-32
SKB Annual Report 1988
Including Summaries of Technical Reports Issued during 1988
Stockholm, May 1989

1989
TR 89-40
SKB Annual Report 1989
Including Summaries of Technical Reports Issued during 1989
Stockholm, May 1990

1990
TR 90-46
SKB Annual Report 1990
Including Summaries of Technical Reports Issued during 1990
Stockholm, May 1991

1991
TR 91-64
SKB Annual Report 1991
Including Summaries of Technical Reports Issued during 1991
Stockholm, April 1992

1992
TR 92-46
SKB Annual Report 1992
Including Summaries of Technical Reports Issued during 1992
Stockholm, May 1993

Technical Reports
List of SKB Technical Reports 1993

TR 93-01
Stress redistribution and void growth in butt-welded canisters for spent nuclear fuel
B L Josefson[1], L Karlsson[2], H-Å Häggblad[2]
[1] Division of Solid Mechanics, Chalmers University of Technology, Göteborg, Sweden
[2] Division of Computer Aided Design, Luleå University of Technology, Luleå, Sweden
February 1993

TR 93-02
Hydrothermal field test with French candidate clay embedding steel heater in the Stripa mine
R Pusch[1], O Karnland[1], A Lajudie[2], J Lechelle[2], A Bouchet[3]
[1] Clay Technology AB, Sweden
[2] CEA, France
[3] Etude Recherche Materiaux (ERM), France
December 1992

TR 93-03
MX 80 clay exposed to high temperatures and gamma radiation
R Pusch[1], O Karnland[1], A Lajudie[2], A Decarreau[3],
[1] Clay Technology AB, Sweden
[2] CEA, France
[3] Univ. de Poitiers, France
December 1992

TR 93-04
Project on Alternative Systems Study (PASS).
Final report
October 1992

TR 93-05
Studies of natural analogues and geological systems.
Their importance to performance assessment.
Fredrik Brandberg[1], Bertil Grundfelt[1], Lars Olof Höglund[1], Fred Karlsson[2],
Kristina Skagius[1], John Smellie[3]
[1] KEMAKTA Konsult AB
[2] SKB
[3] Conterra AB
April 1993

TR 93-06
Mineralogy, geochemistry and petrophysics of red coloured granite adjacent to fractures
Thomas Eliasson
Chalmers University of Technology and University of Göteborg, Department of Geology, Göteborg, Sweden
March 1993

TR 93-07
Modelling the redox front movement in a KBS-3 nuclear waste repository
L Romero, L Moreno, I Neretnieks
Department of Chemical Engineering,
Royal Institute of Technology, Stockholm, Sweden
May 1993

TR 93-08
Äspö Hard Rock Laboratory
Annual Report 1992
SKB
April 1993

TR 93-09
Verification of the geostatistical inference code INFERENS, Version 1.1, and demonstration using data from Finnsjön
Joel Geier
Golder Geosystem AB, Uppsala
June 1993